Variety of disk wind-driven explosions in massive rotating stars

Ludovica Crosato Menegazzi

Collaborators: Sho Fujibayashi, Masaru Shibata

MAX-PLANCK-INSTITUT
FÜR GRAVITATIONSPHYSIK
(Albert-Einstein-Institut)

DESY.

TeVPA2026, Tendo, 3 September

TeV Particle Astrophysics
TeVPA 2026
Tendo
Japan
August 30 - September 4, 2026

Fate of massive stars

Massive star

$$M_{\mathrm{ZAMS}} \gtrsim 8\ M_{\odot}$$

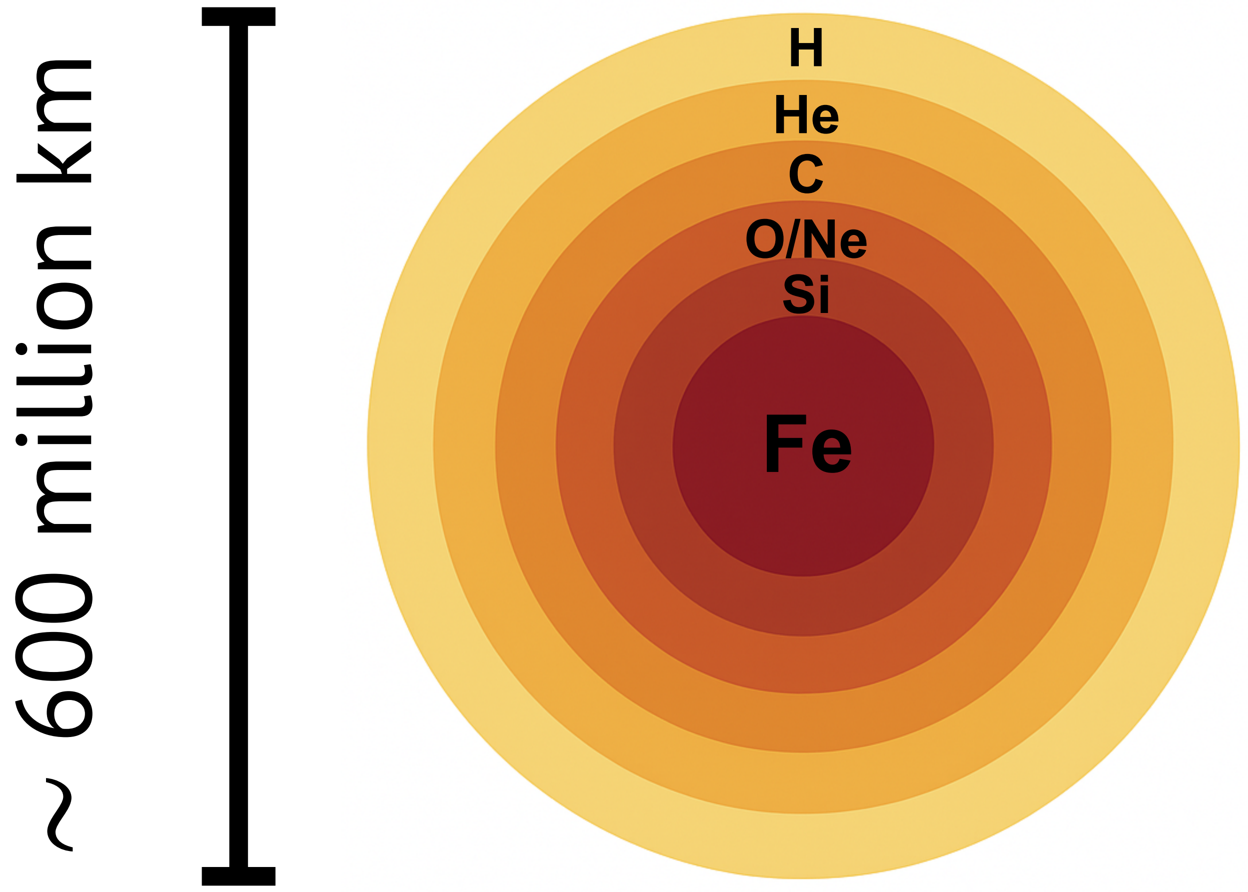

Gravitational core-collapse

Fate of massive stars

Massive star

$M_{\mathrm{ZAMS}} \gtrsim 8\, M_{\odot}$

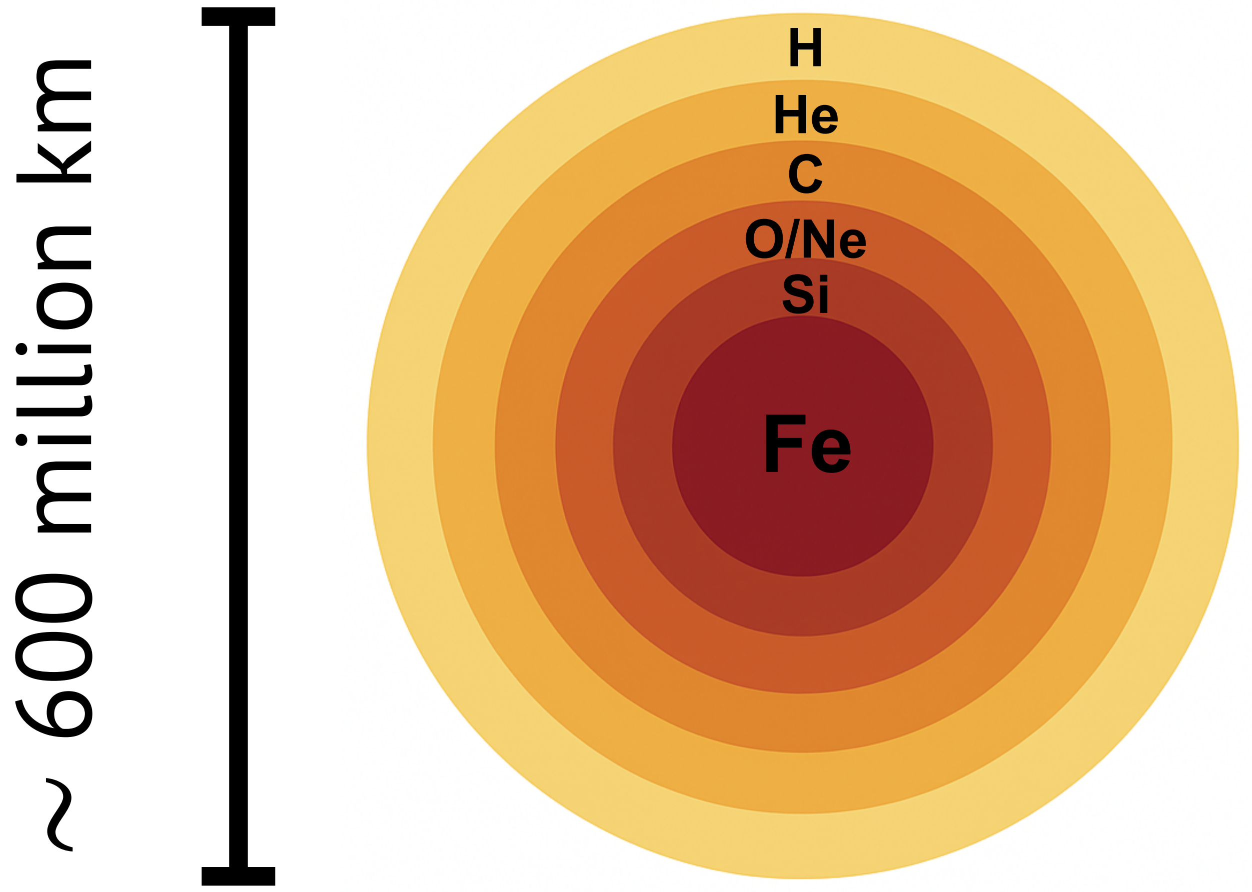

Gravitational core-collapse

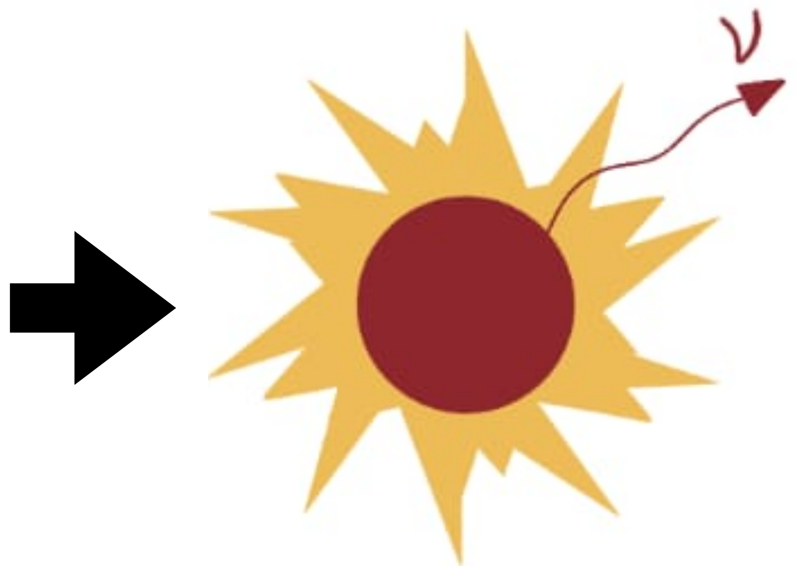

Core bounce

Fate of massive stars

Massive star

$M_{\rm ZAMS} \gtrsim 8\ M_\odot$

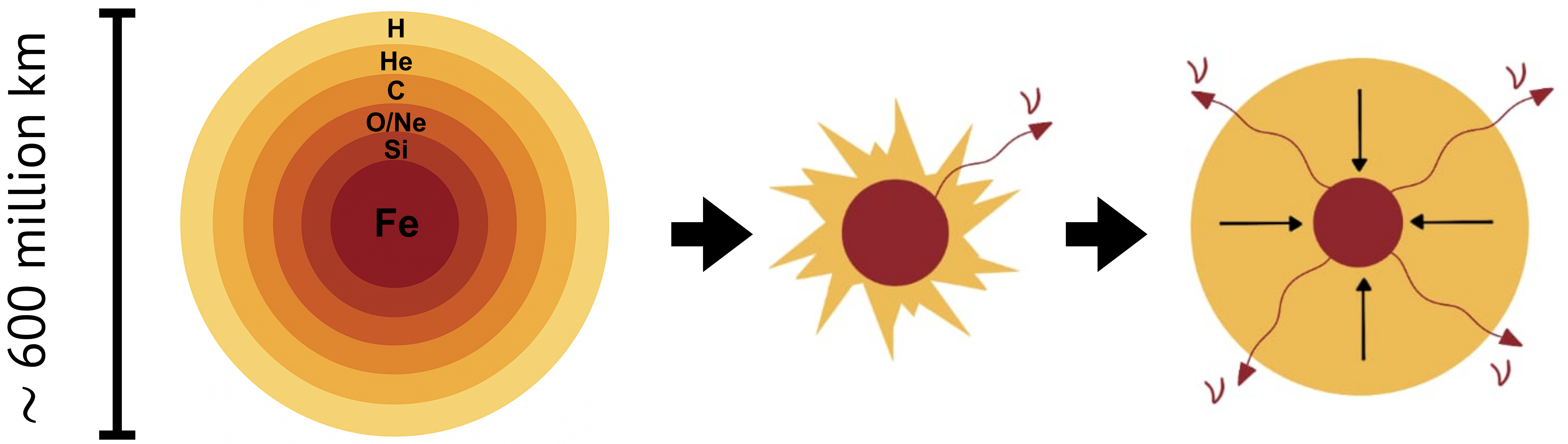

Gravitational core-collapse

Core bounce

Proto-neutron star

Fate of massive stars

Massive star

$M_{\rm ZAMS} \gtrsim 8\ M_\odot$

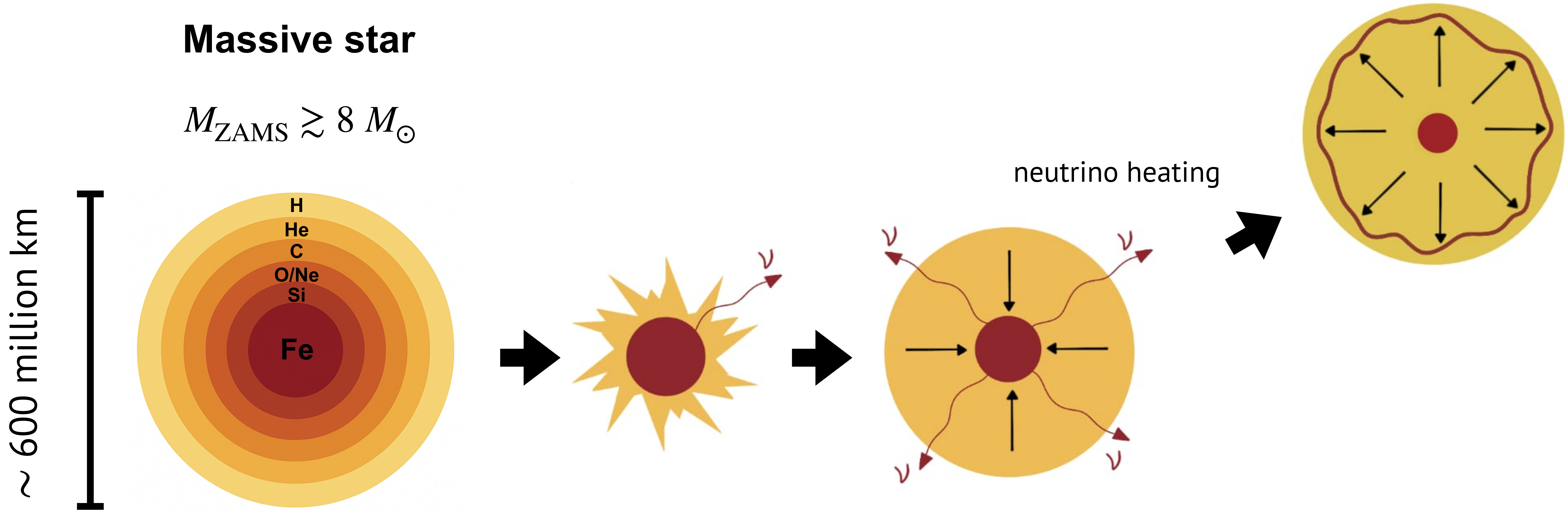

Gravitational core-collapse

Core bounce

Proto-neutron star

Fate of massive stars

Massive star

$M_{\rm ZAMS} \gtrsim 8\ M_{\odot}$

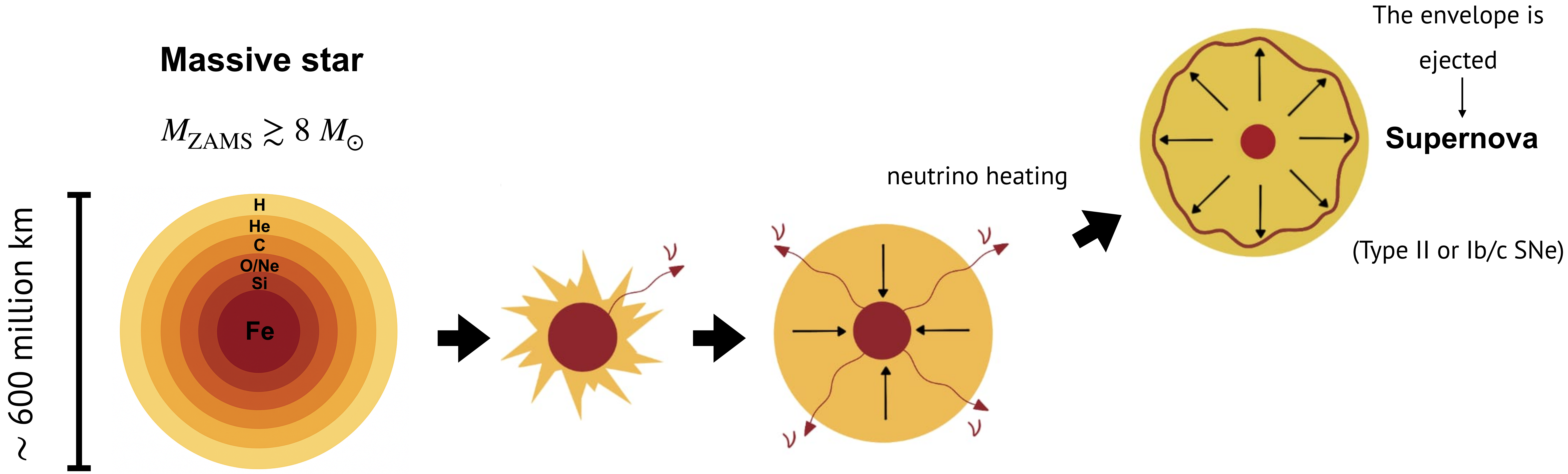

Gravitational core-collapse

Core bounce

Proto-neutron star

Fate of massive stars

Massive star

$M_{\rm ZAMS} \gtrsim 8\, M_\odot$

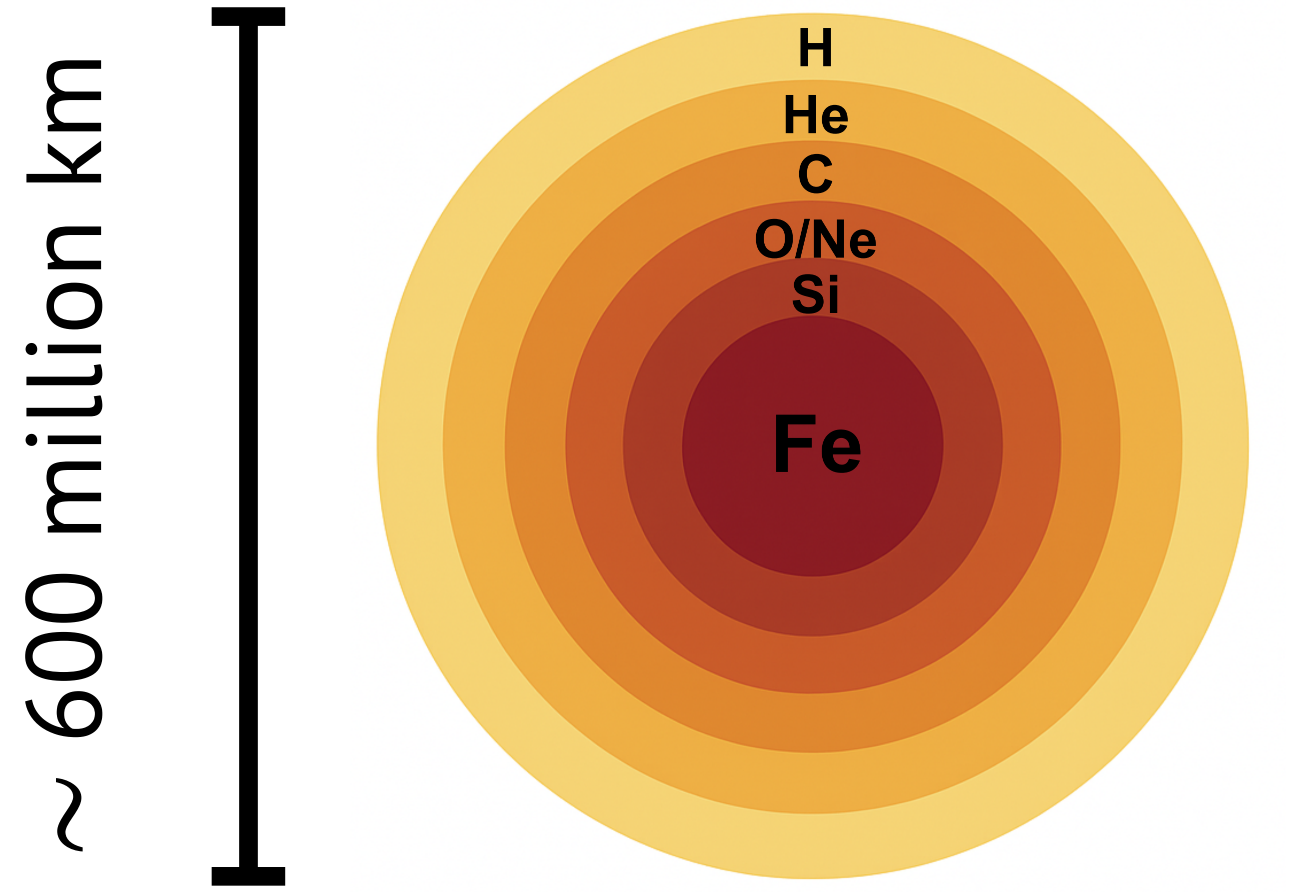

Gravitational core-collapse

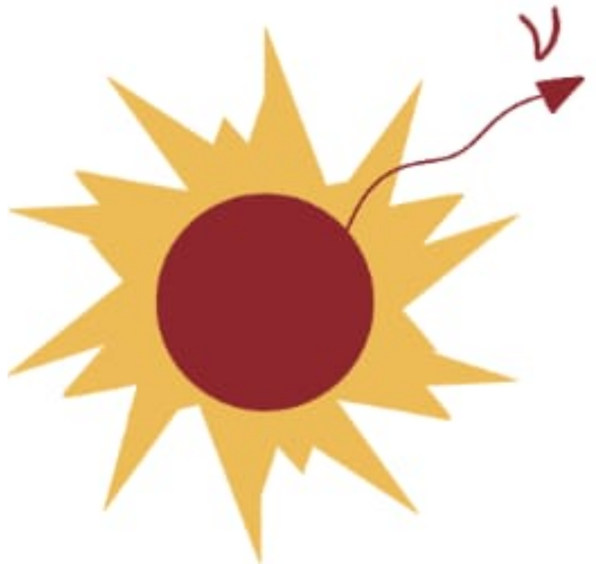

Core bounce

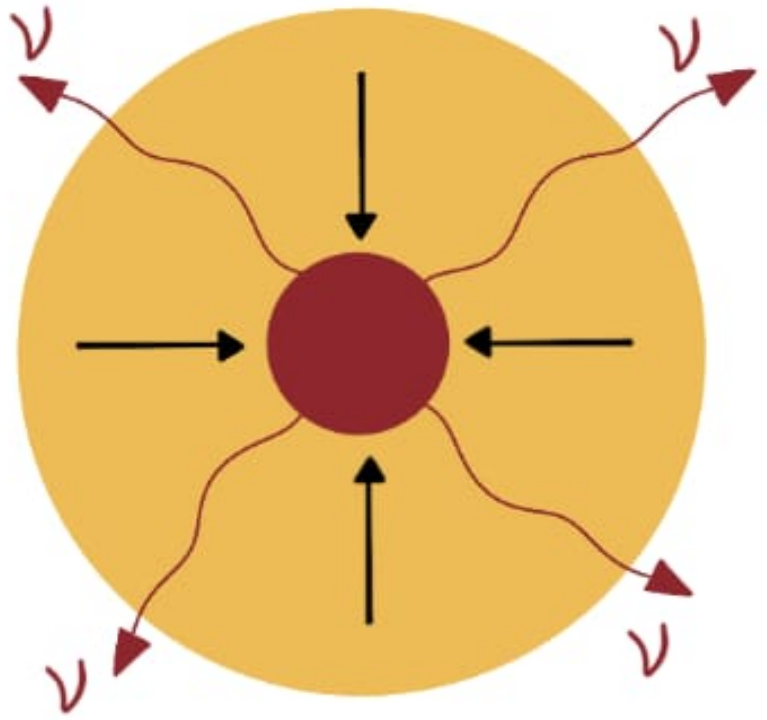

Proto-neutron star

neutrino heating

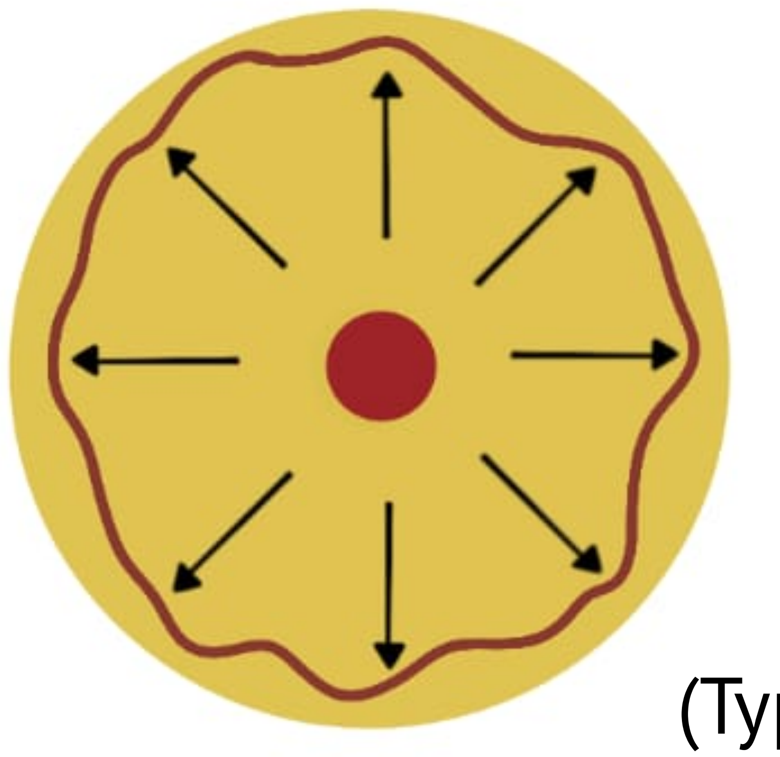

The envelope is ejected

Supernova

(Type II or Ib/c SNe)

- Moderate progenitor mass
- Low compactness $(\xi_{2.5} < 0.45)$

$$\xi_{M/M_\odot} = \frac{M/M_\odot}{R(M)/1000\text{km}}$$

- High metallicity

Fate of massive stars

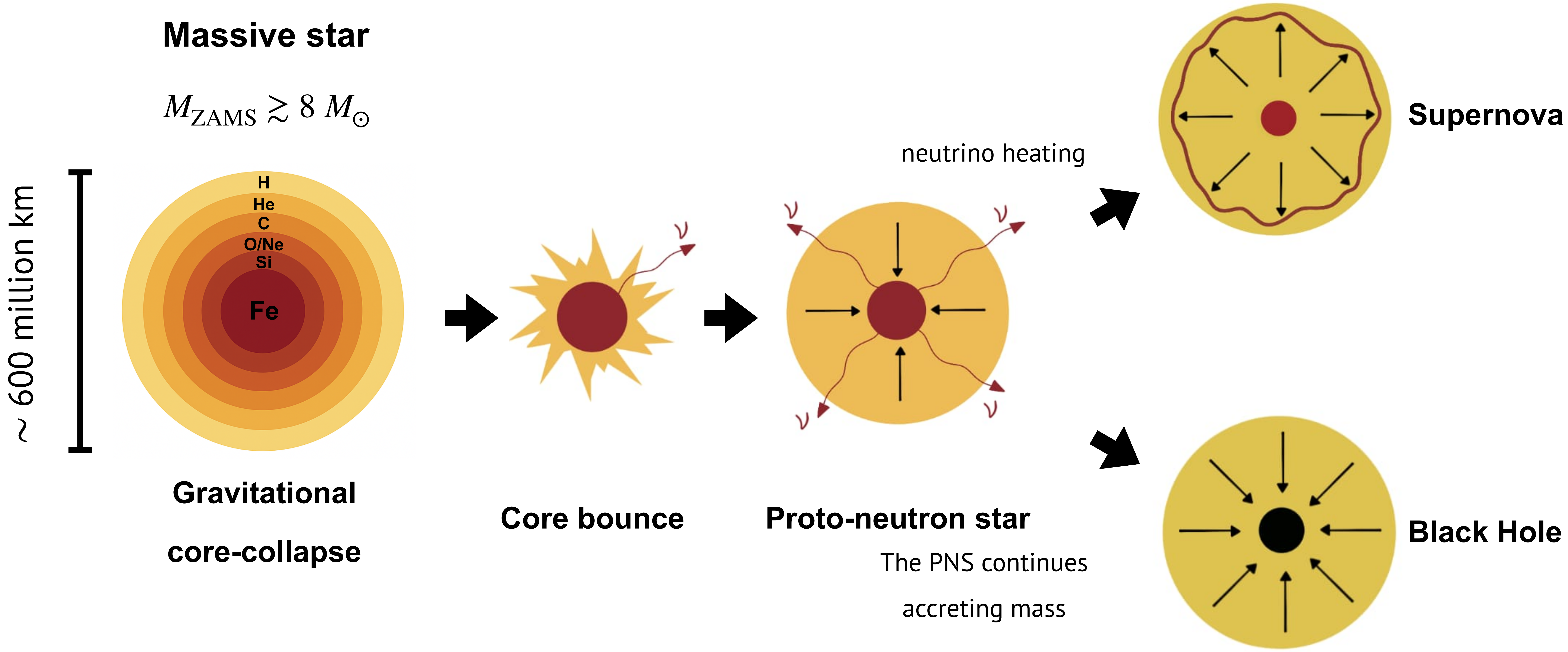

Fate of massive stars

Massive star

$M_{\rm ZAMS} \gtrsim 8\ M_\odot$

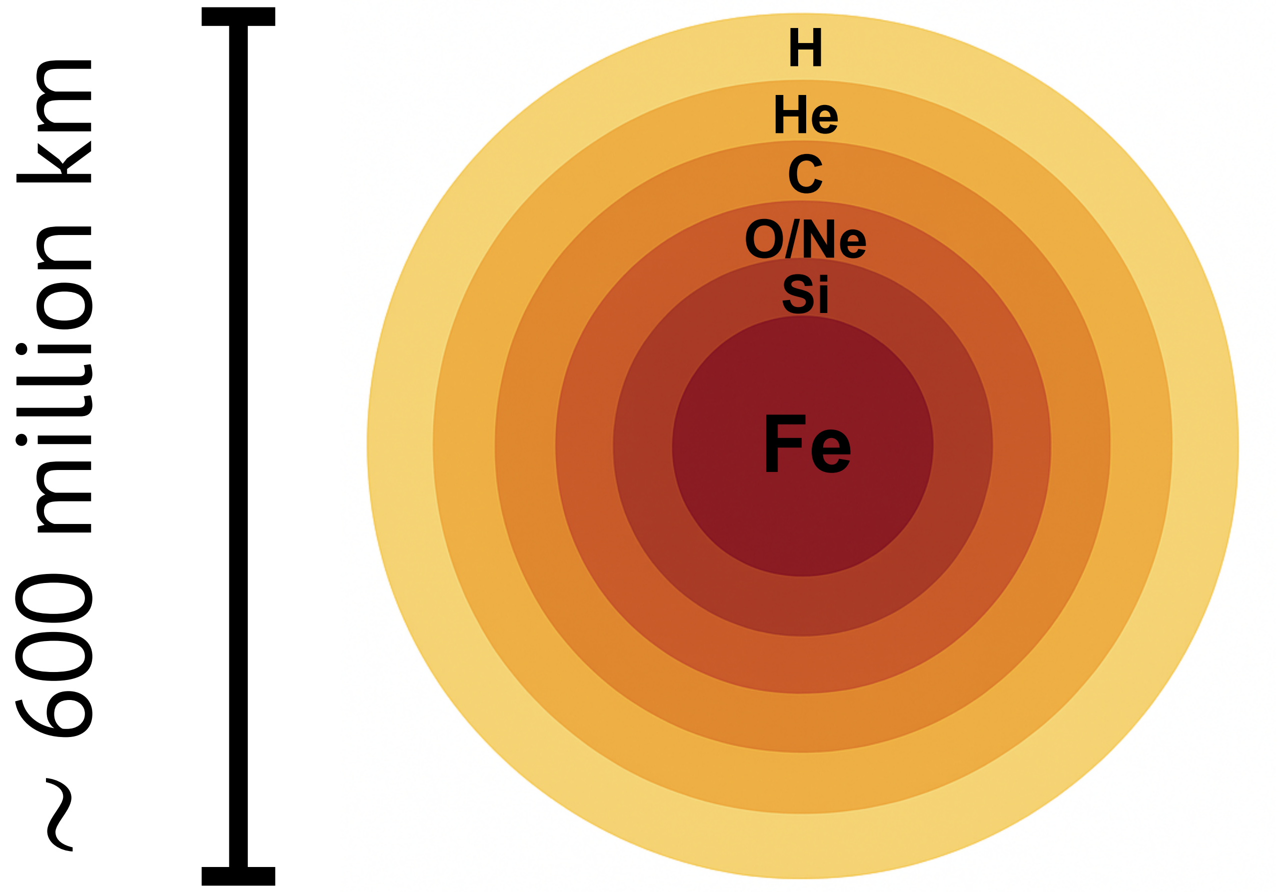

Gravitational core-collapse

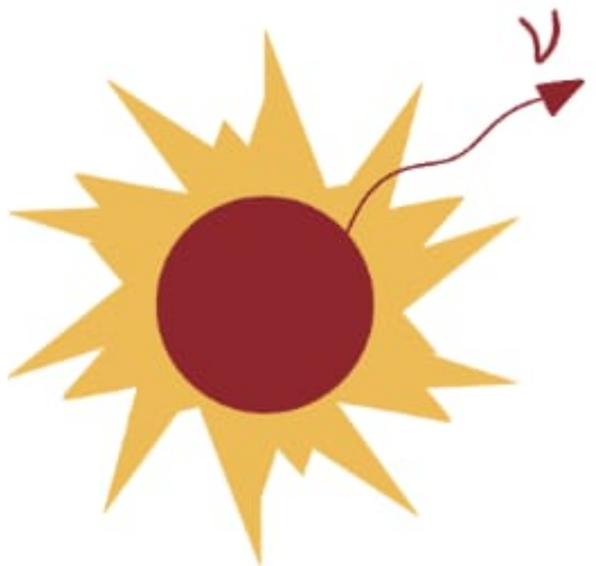

Core bounce

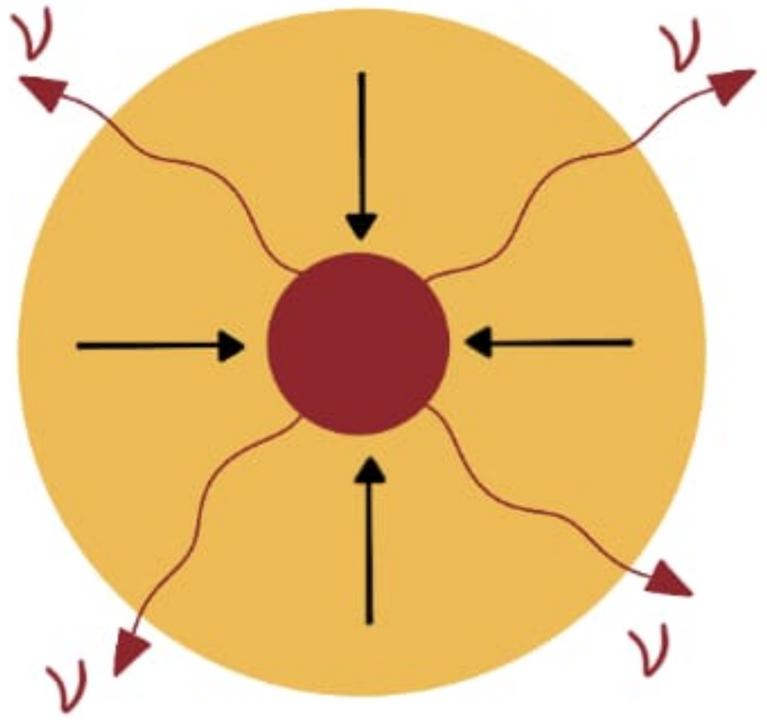

Proto-neutron star

The PNS continues accreting mass

- Higher progenitor mass
  $M_{\rm ZAMS} \gtrsim 16 - 20\ M_\odot$
  Sukhbold &Woosley (2014)
- High compactness $(\xi_{2.5} > 0.45)$
  Ertl et al. (2016)
  Müller et al. (2016)
- Low metallicity
- Rapid mass accretion rate

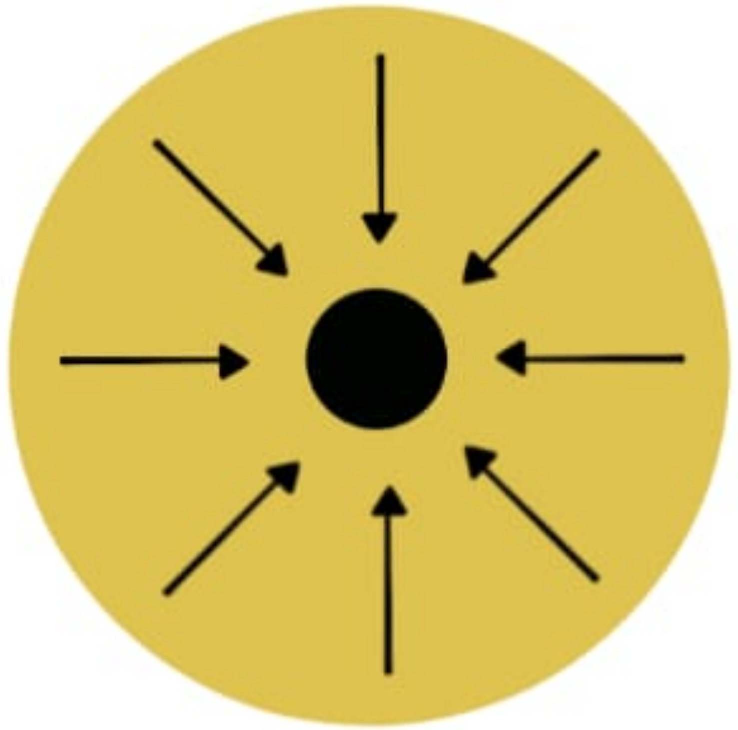

Black Hole

Association between failed SNe and GRBs

$M \gtrsim 16 - 20\ M_\odot$

$\xi_{2.5} > 0.45$

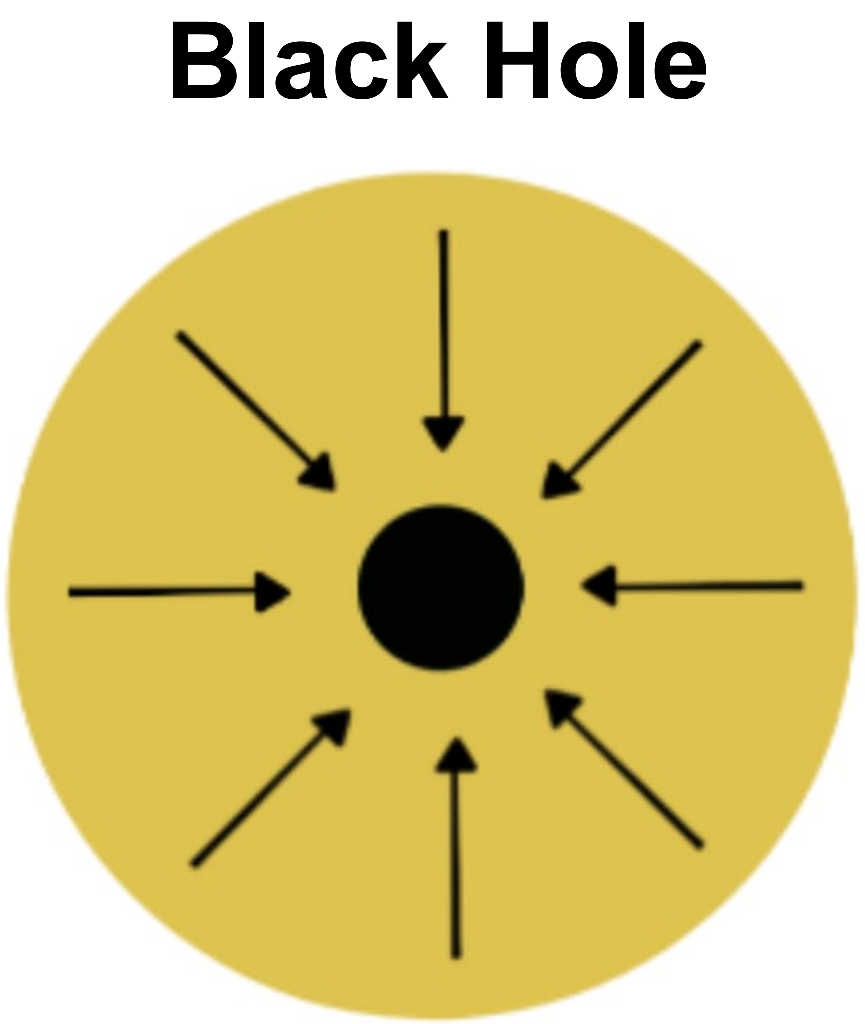

Association between failed SNe and GRBs

Black Hole

$M \gtrsim 16 - 20\ M_\odot$

$\xi_{2.5} > 0.45$

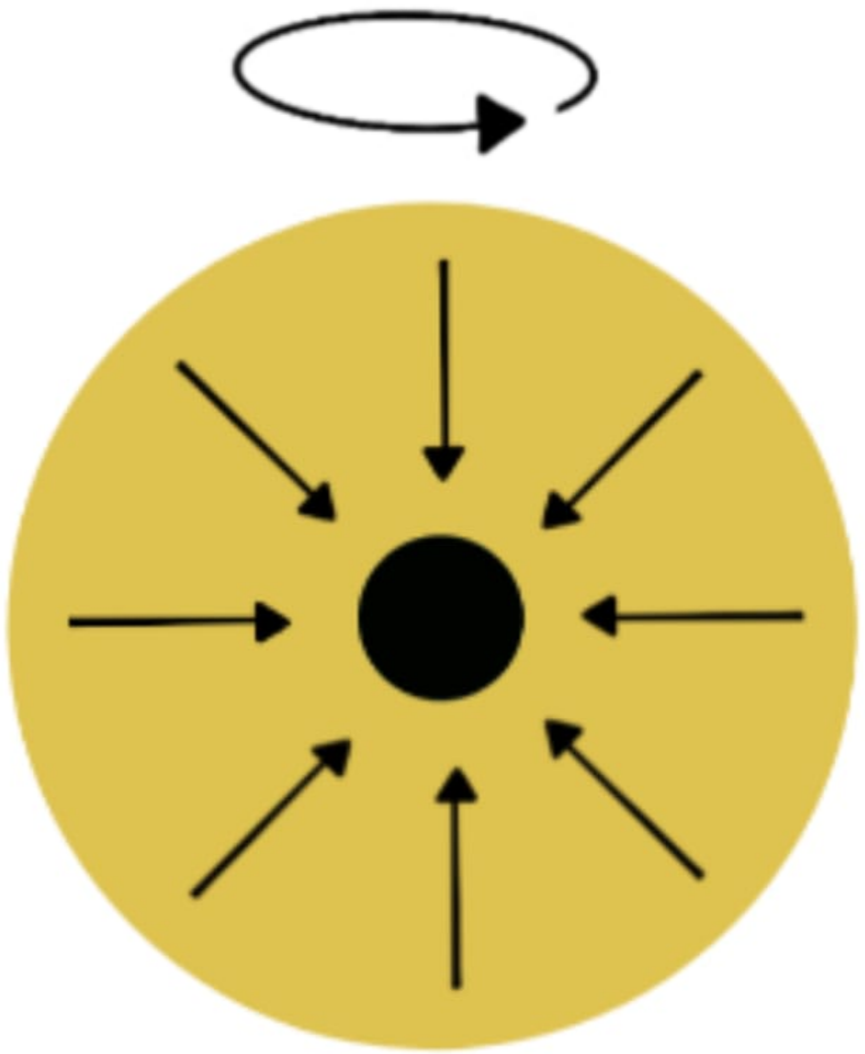

+ rotation

Association between failed SNe and GRBs

Black Hole

$M \gtrsim 16 - 20\ M_\odot$

$\xi_{2.5} > 0.45$

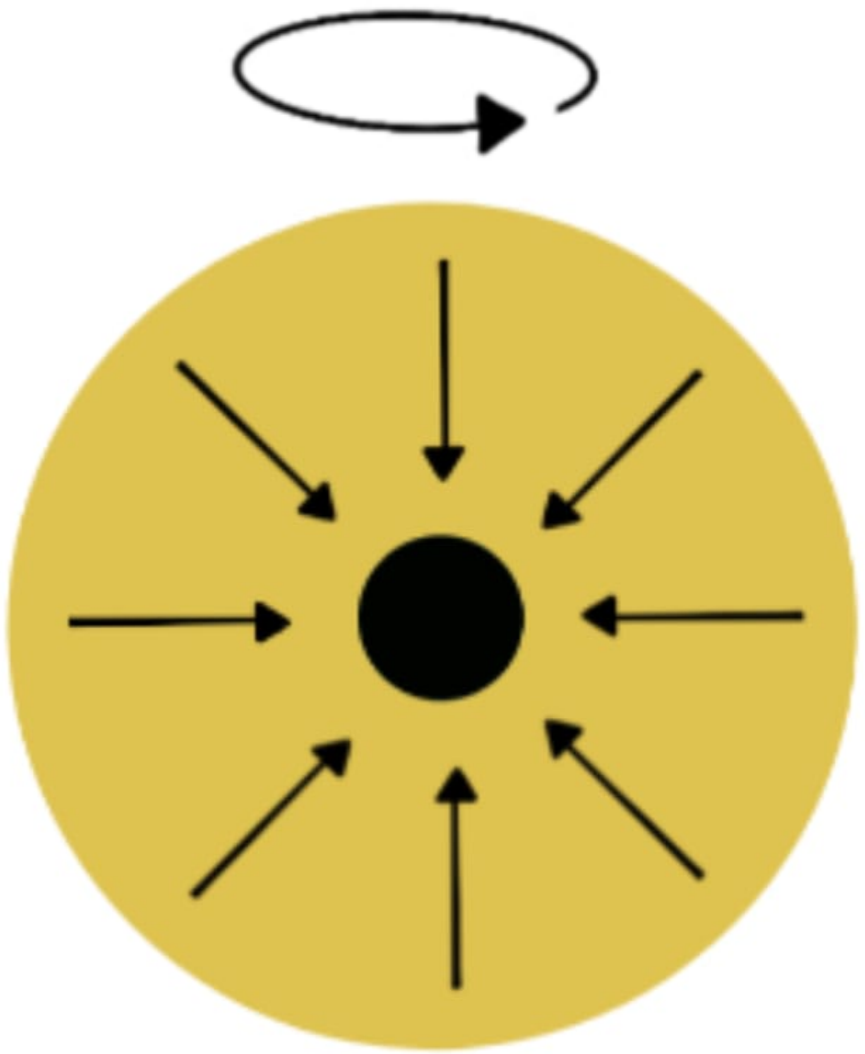

+ rotation

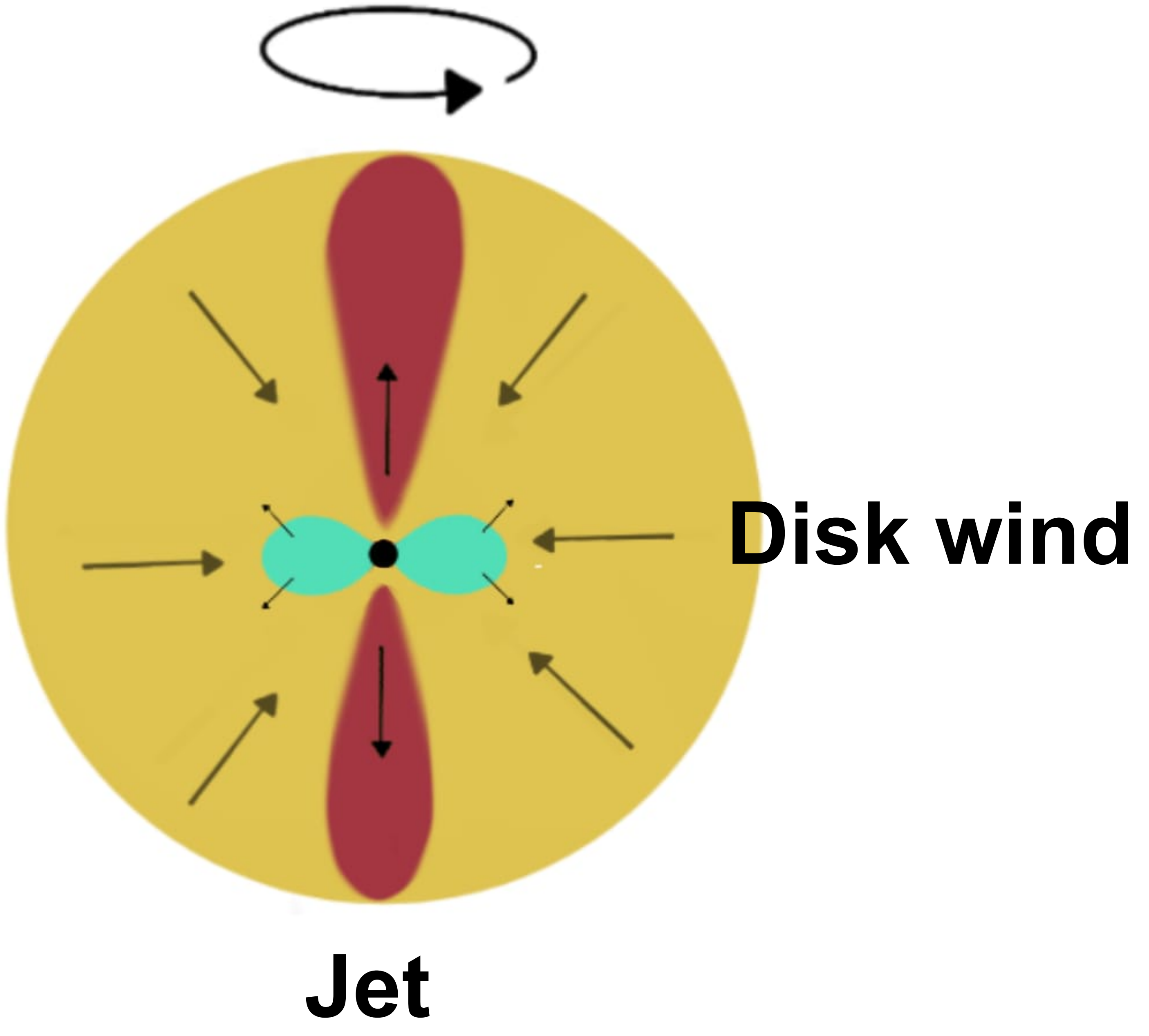

Association between failed SNe and GRBs

Black Hole

$M \gtrsim 16 - 20\ M_\odot$

$\xi_{2.5} > 0.45$

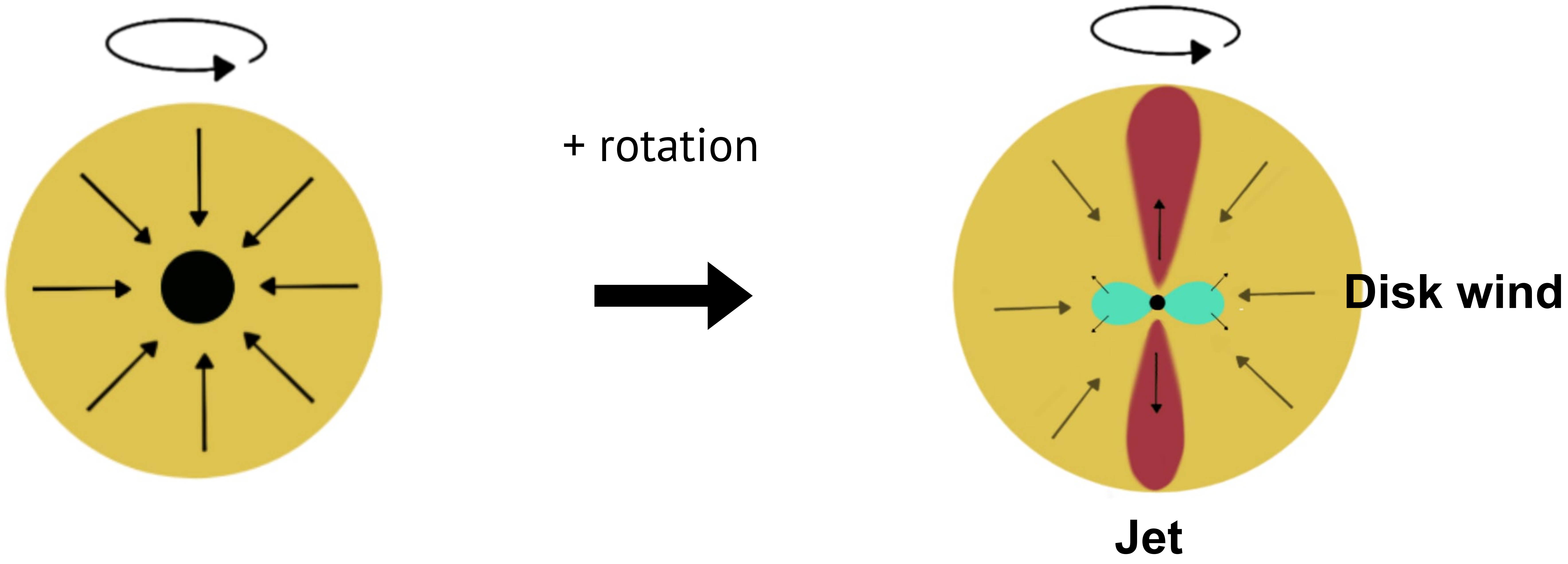

- Spectroscopic and Photometric observations associated with Type Ic-SNe

(Mészáros 2006)

Association between failed SNe and GRBs

Black Hole

$M \gtrsim 16 - 20\ M_\odot$

$\xi_{2.5} > 0.45$

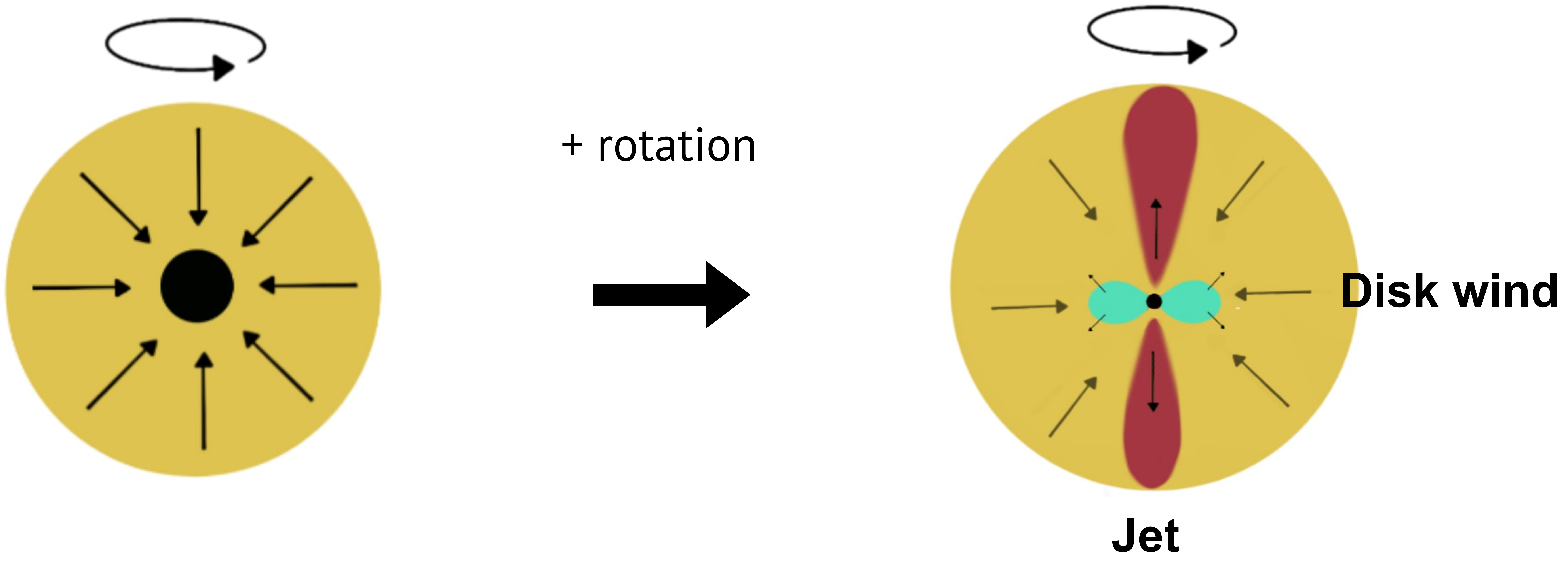

- Spectroscopic and Photometric observations associated with Type Ic-SNe (Mészáros 2006)

- Massive Type Ic-SNe can be accounted for the huge amount $^{56}\mathrm{Ni}$ produced ($M_{\mathrm{Ni}} > 0.1\,M_\odot$) (Cano & al. 2017)

Association between failed SNe and GRBs

Black Hole

$M \gtrsim 16 - 20\ M_\odot$

$\xi_{2.5} > 0.45$

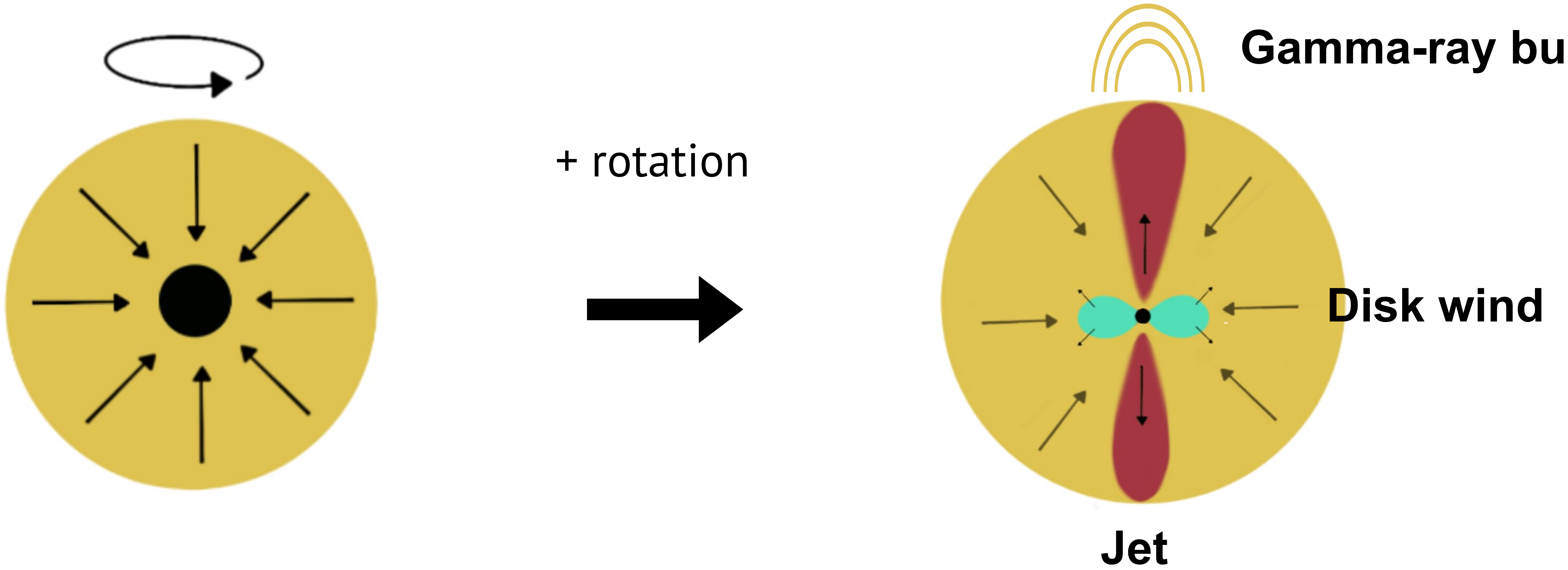

- Spectroscopic and Photometric observations associated with Type Ic-SNe (Mészáros 2006)
- Massive Type Ic-SNe can be accounted for the huge amount ^{56}Ni produced ($M_{\rm Ni} > 0.1\, M_\odot$) (Cano & al. 2017)
- Formation of highly relativistic jets (MacFadyen & Woosley 1999,T. Piran & al. 2019)

Scientific motivation and Objectives

Open questions

- Several models proposed as central engine of long GRBs
- Non strict threshold between successful and failed SNe
- Dim-observed (non-standard) CCSNe associated with GRBs
- ^{56}Ni production can constrain central engine properties
- High ^{56}Ni production still not fully understood

Scientific motivation and Objectives

Open questions

- Several models proposed as central engine of long GRBs
- Non strict threshold between successful and failed SNe
- Dim-observed (non-standard) CCSNe associated with GRBs
- ^{56}Ni production can constrain central engine properties
- High ^{56}Ni production still not fully understood

Goal

Investigate the ejecta properties and the ^{56}Ni production to constrain the explosion mechanism and assess the viability of failed SNe as GRBs progenitors

Scientific motivation and Objectives

Open questions

- Several models proposed as central engine of long GRBs
- Non strict threshold between successful and failed SNe
- Dim-observed (non-standard) CCSNe associated with GRBs
- ^{56}Ni production can constrain central engine properties
- High ^{56}Ni production still not fully understood

Goal

Investigate the ejecta properties and the ^{56}Ni production to constrain the explosion mechanism and assess the viability of failed SNe as GRBs progenitors

What's new in this work

- General central engine model
- Systematic multi-dimensional simulations
- Exploration of a broader parameter space than in previous works

The computational method

Simulating failed CCSNe using the open-source hydrodynamic infrastructure **Athena++**

Code overview:

Solving the hydrodynamics of the star

Hydrodynamics solver

Riemann solver: HLL

2D spherical-polar coordinates

Axisymmetric geometry

Time integration

Second-order Van Leer predictor-corrector scheme

The computational method

Simulating failed CCSNe using the open-source hydrodynamic infrastructure **Athena++**

Code overview:

Solving the hydrodynamics of the star

Hydrodynamics solver

Riemann solver: HLL

2D spherical-polar coordinates

Axisymmetric geometry

Time integration

Second-order Van Leer predictor-corrector scheme

New physics implemented

1. Realistic **Equation Of State**
2. **Gravity solver** (for the self gravity)
3. **Boundary condition** for the outflow launching

Simulating failed SNe

$M \gtrsim 16 - 20\ M_\odot$

$\xi_{2.5} > 0.45$

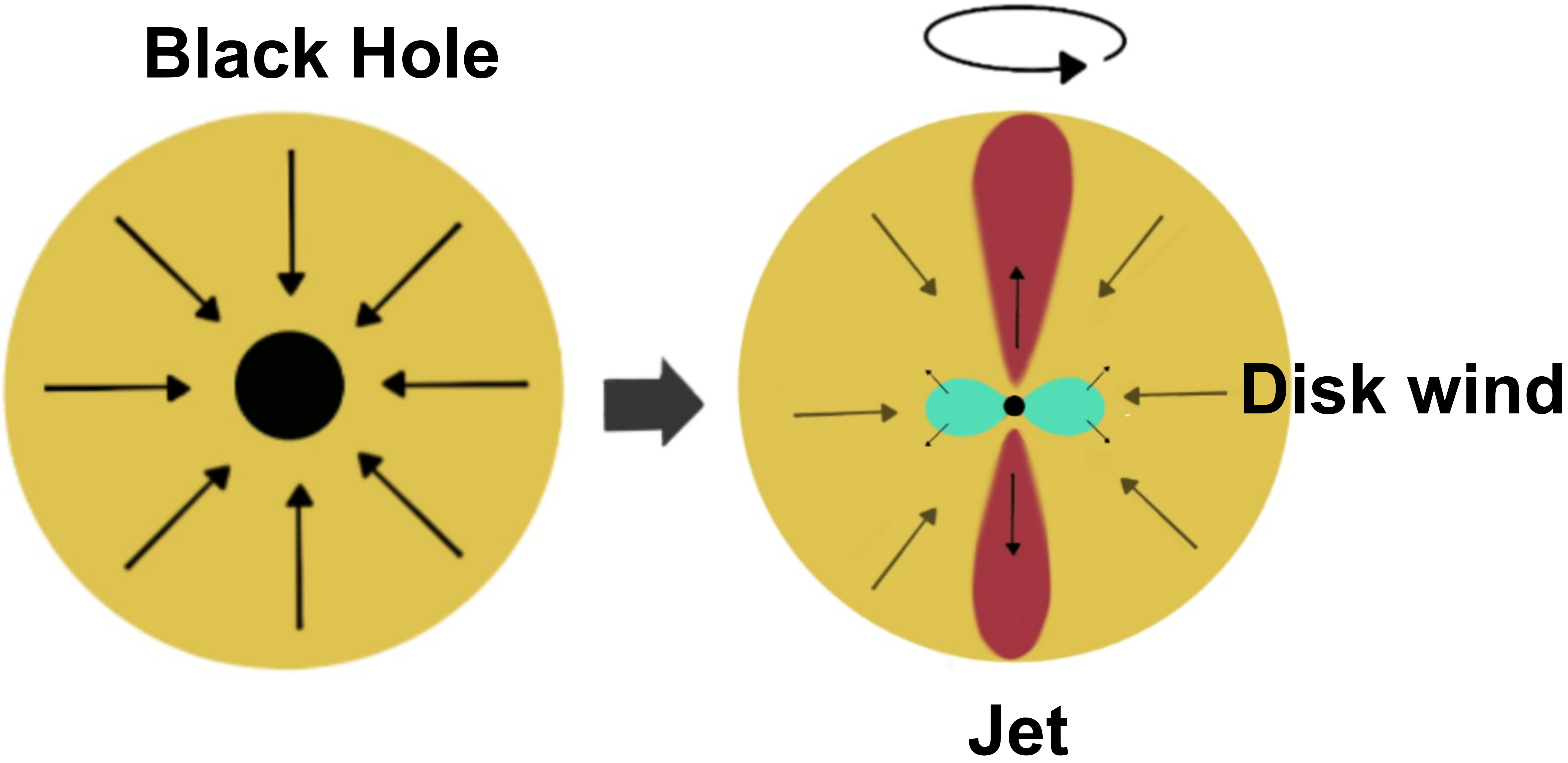

Our setup

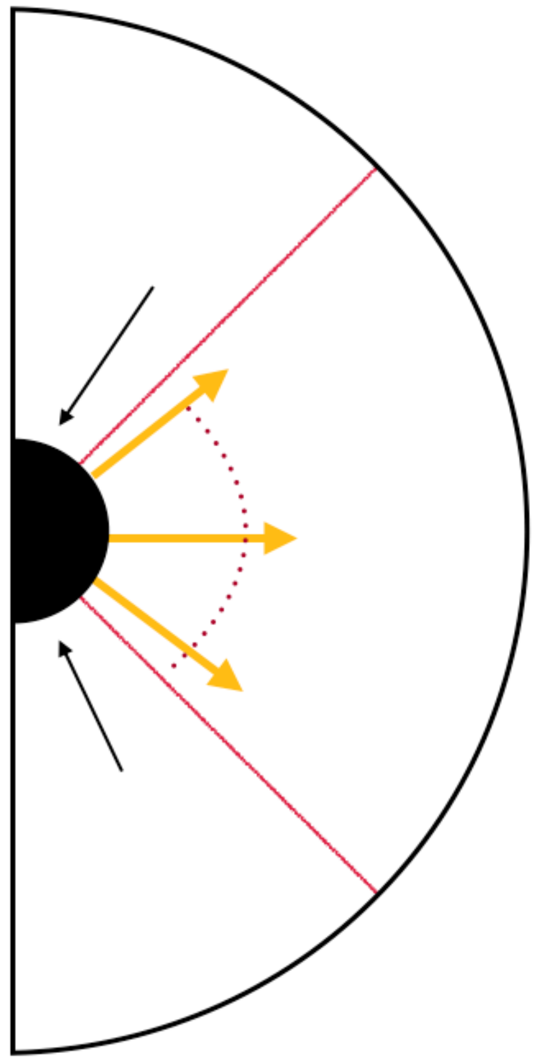

Simulation setup and physical assumption

Explosion properties and ^{56}Ni production studied as function of wind injection and progenitor structure

Configuration

- 2D axisymmetric non-relativistic simulations using Athena++
- Central engine excised at inner boundary $r_{in} = 1000$ km
- Computational domain extended beyond the stellar surface to $r_{out} = 3.34 \times 10^{10}$ cm
- Self-gravity computed solving the gravitational potential Φ

Progenitors

- Rapidly rotating progenitors
  Aguilera-Dena et al.,2020; Woosley&Heger,2006
- Oxygen based equation of state

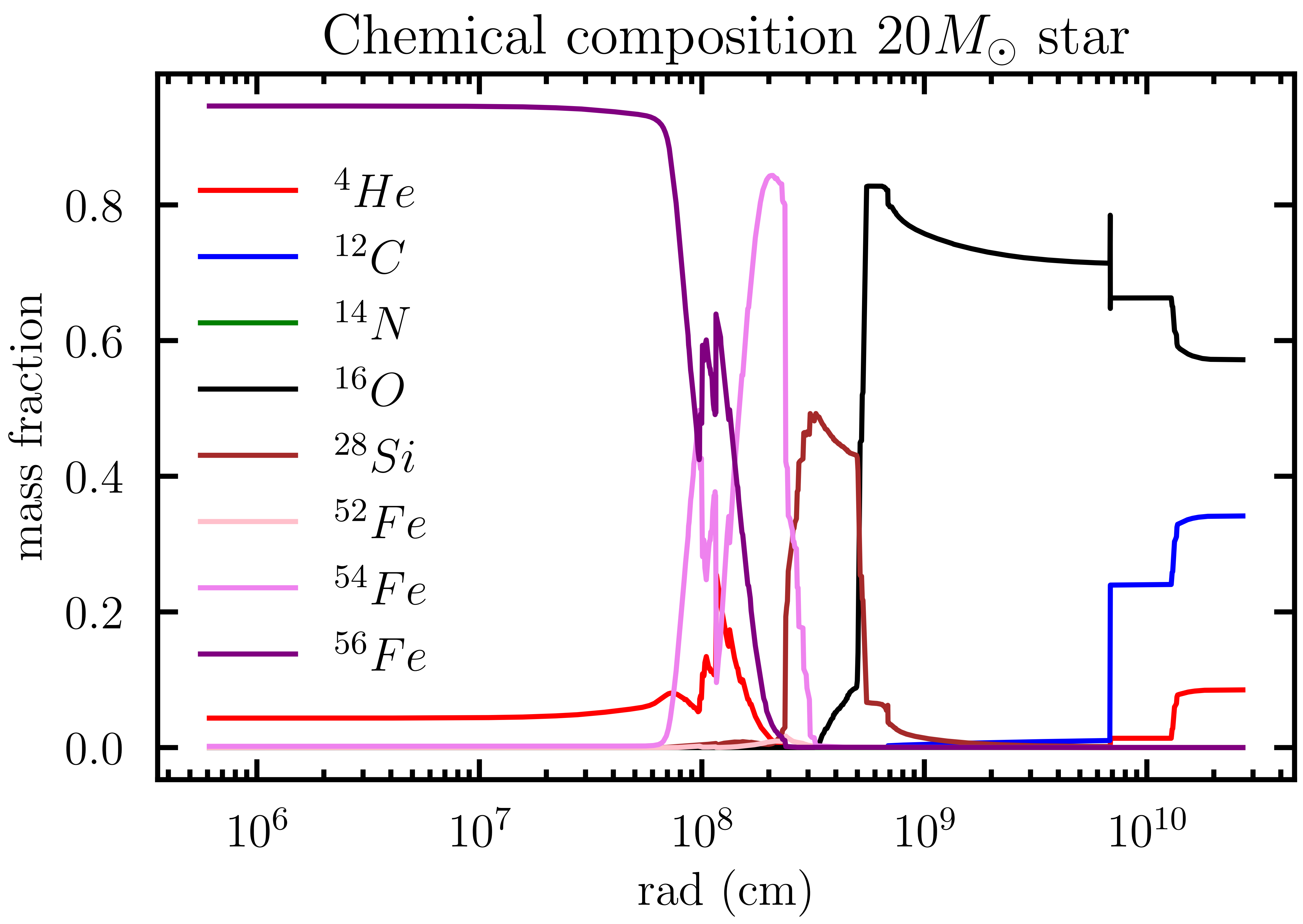

Pre-collapse composition dominated by oxygen

The model of the central engine

$$\frac{dM_{\rm disk}}{dt} = \dot{M}_{\rm fall,disk} - \dot{M}_{\rm acc} - \dot{M}_{\rm wind}$$

$$\frac{dM_{\rm BH}}{dt} = \dot{M}_{\rm fall,BH} + \dot{M}_{\rm acc}$$

$$\frac{dJ_{\rm disk}}{dt} = \dot{J}_{\rm fall,disk} - \dot{J}_{\rm acc} - \dot{J}_{\rm wind}$$

$$\frac{dJ_{\rm BH}}{dt} = \dot{J}_{\rm fall,BH} + \dot{J}_{\rm acc}$$

The model of the central engine

$$\frac{dM_{\rm disk}}{dt} = \dot{M}_{\rm fall,disk} - \dot{M}_{\rm acc} - \dot{M}_{\rm wind}$$

$$\frac{dM_{\rm BH}}{dt} = \dot{M}_{\rm fall,BH} + \dot{M}_{\rm acc}$$

$$\frac{dJ_{\rm disk}}{dt} = \dot{J}_{\rm fall,disk} - \dot{J}_{\rm acc} - \dot{J}_{\rm wind}$$

$$\frac{dJ_{\rm BH}}{dt} = \dot{J}_{\rm fall,BH} + \dot{J}_{\rm acc}$$

The model of the central engine

$$\frac{dM_{\rm disk}}{dt} = \dot{M}_{\rm fall,disk} - \dot{M}_{\rm acc} - \dot{M}_{\rm wind}$$

$$\frac{dM_{\rm BH}}{dt} = \dot{M}_{\rm fall,BH} + \dot{M}_{\rm acc}$$

$$\frac{dJ_{\rm disk}}{dt} = \dot{J}_{\rm fall,disk} - \dot{J}_{\rm acc} - \dot{J}_{\rm wind}$$

$$\frac{dJ_{\rm BH}}{dt} = \dot{J}_{\rm fall,BH} + \dot{J}_{\rm acc}$$

Accretion term:

$$\begin{cases} \dot{M}_{\rm acc} = \dfrac{M_{\rm disk}}{t_{\rm acc}} \\ \dot{J}_{\rm acc} = \dfrac{M_{\rm disk}}{t_{\rm acc}} j_{\rm ISCO} \end{cases}$$

The model of the central engine

$$\frac{dM_{\rm disk}}{dt} = \dot{M}_{\rm fall,disk} - \dot{M}_{\rm acc} - \dot{M}_{\rm wind}$$

$$\frac{dM_{\rm BH}}{dt} = \dot{M}_{\rm fall,BH} + \dot{M}_{\rm acc}$$

$$\frac{dJ_{\rm disk}}{dt} = \dot{J}_{\rm fall,disk} - \dot{J}_{\rm acc} - \dot{J}_{\rm wind}$$

$$\frac{dJ_{\rm BH}}{dt} = \dot{J}_{\rm fall,BH} + \dot{J}_{\rm acc}$$

Wind terms:

$$\begin{cases} \dot{M}_{\rm wind} = \dfrac{M_{\rm disk}}{t_{\rm w}} \\ \dot{J}_{\rm wind} = j_{\rm disk}\dot{M}_{\rm wind} \end{cases}$$

With:

- $t_{\rm w}$ the wind time scale
- $j_{\rm disk} = J_{\rm disk}/M_{\rm disk}$

Setup and parameters

CONDITIONS FOR THE WIND INJECTION

- $\theta_w = \pi/4$ along the equatorial plane

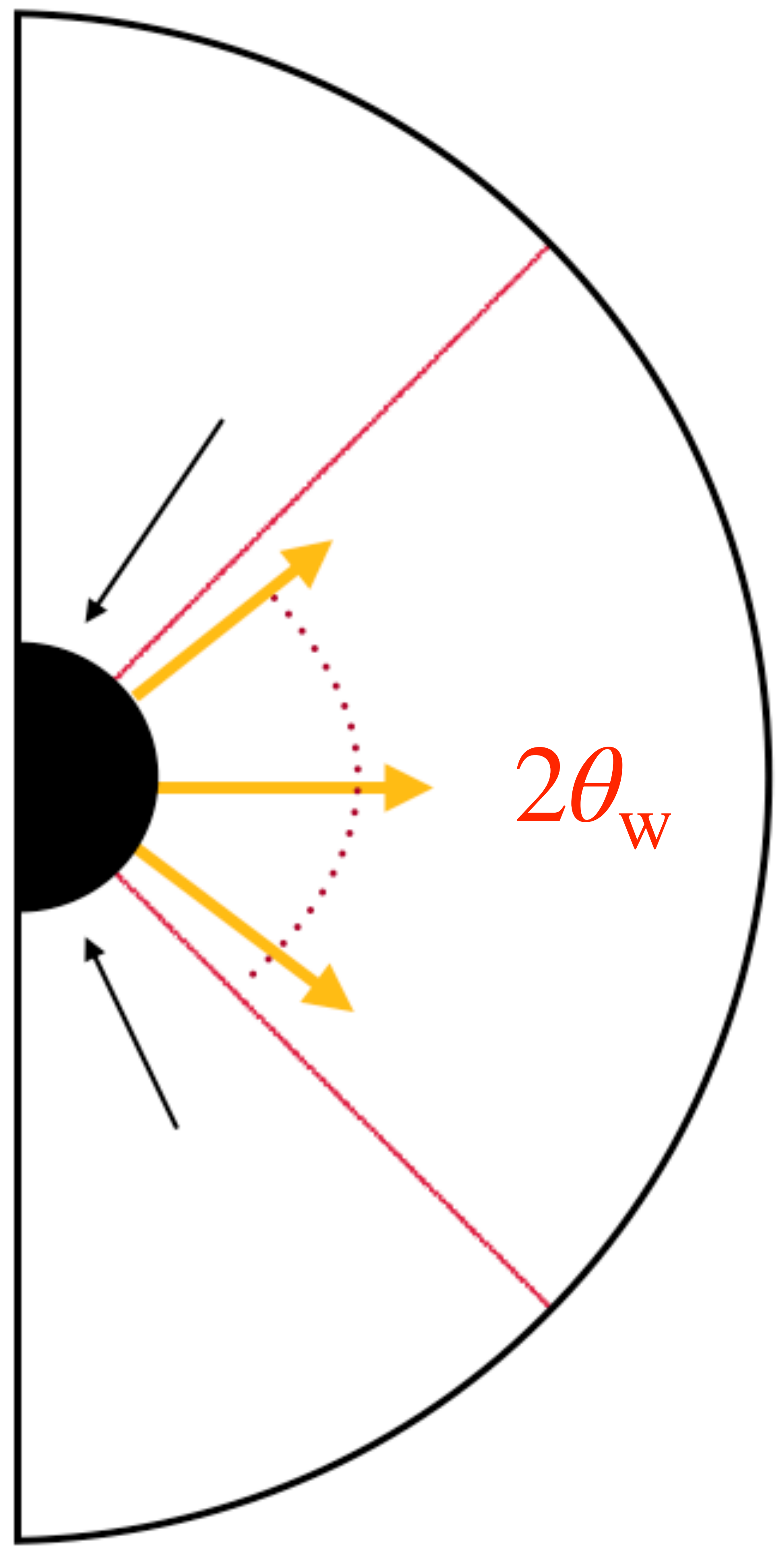

Setup and parameters

CONDITIONS FOR THE WIND INJECTION

- $\theta_\mathrm{w} = \pi/4$ along the equatorial plane
- Parabolic density profile

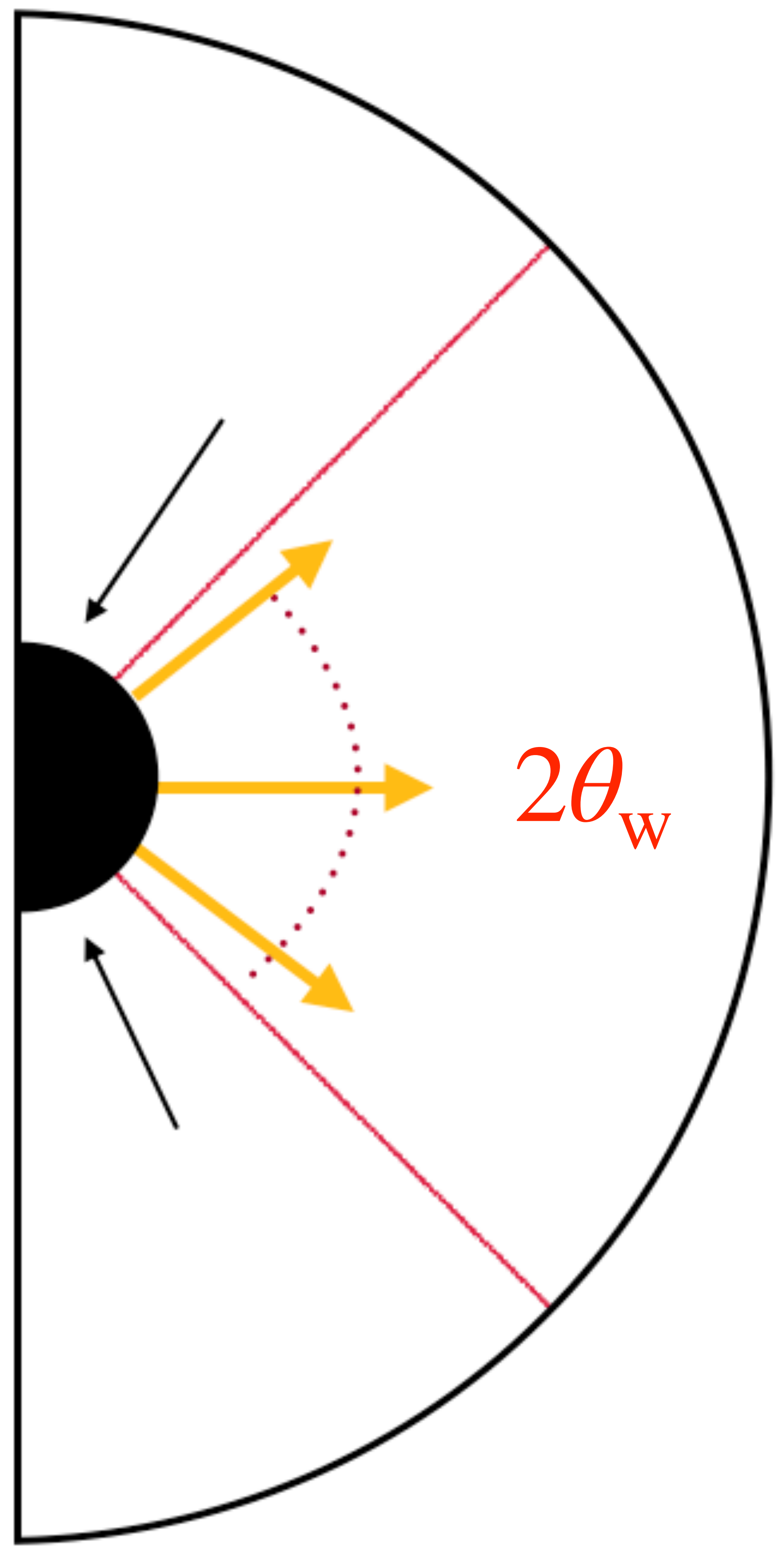

Setup and parameters

CONDITIONS FOR THE WIND INJECTION

- $\theta_{\rm w} = \pi/4$ along the equatorial plane
- Parabolic density profile
- Injected specific energy: $\frac{1}{2}v_{\rm w}^2 + \frac{1}{2}f_{\rm therm}v_{\rm w}^2 + \Phi = \frac{1}{2}\xi^2 v_{\rm esc}^2$

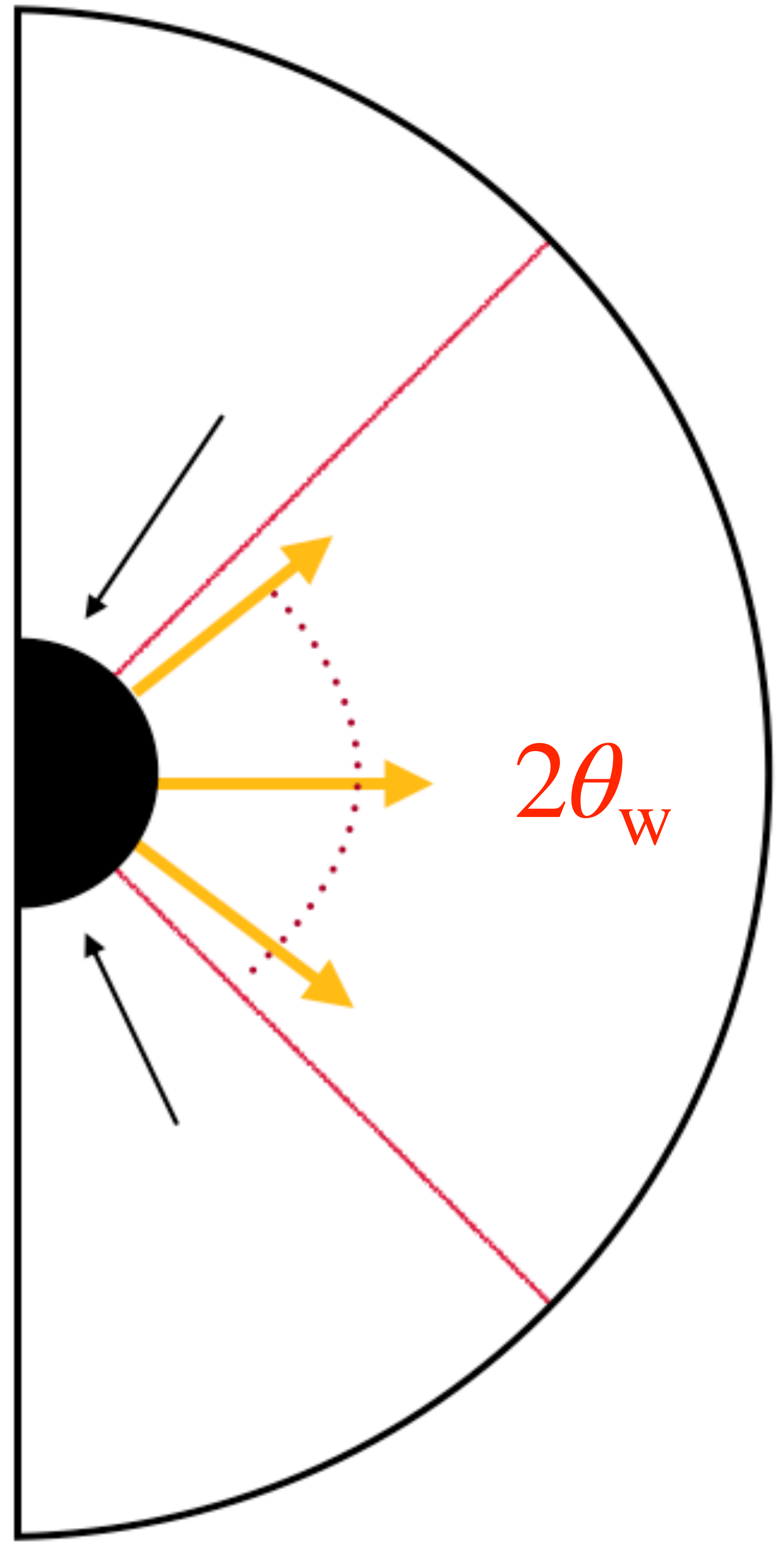

Exploring the wind parameter

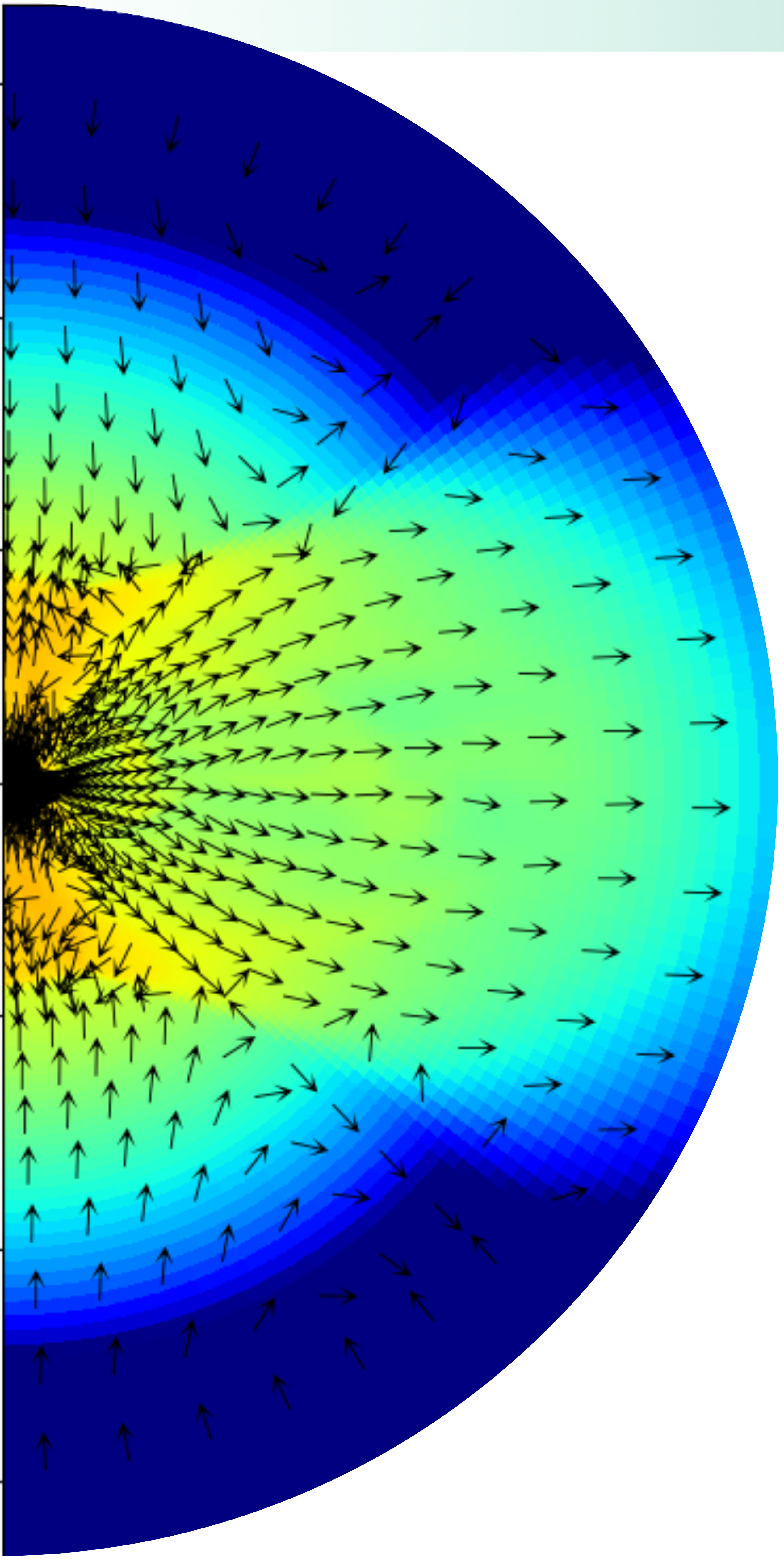

FIXED parameters:

- $M_{\rm ZAMS} = 20\,M_\odot$
- Ω_o

FREE parameters:

- $t_{\rm w} = (0.1, 1.0, 3.16, 10)\,{\rm s}$
- $t_{\rm acc}/t_{\rm w} = (1, 3.16, 10, \infty)$
- $\xi^2 = (0.1, 0.3)$
- $f_{\rm therm} = (0.1, 0.01)$

Evolution of $M_{\rm prog} = 20\,M_\odot$

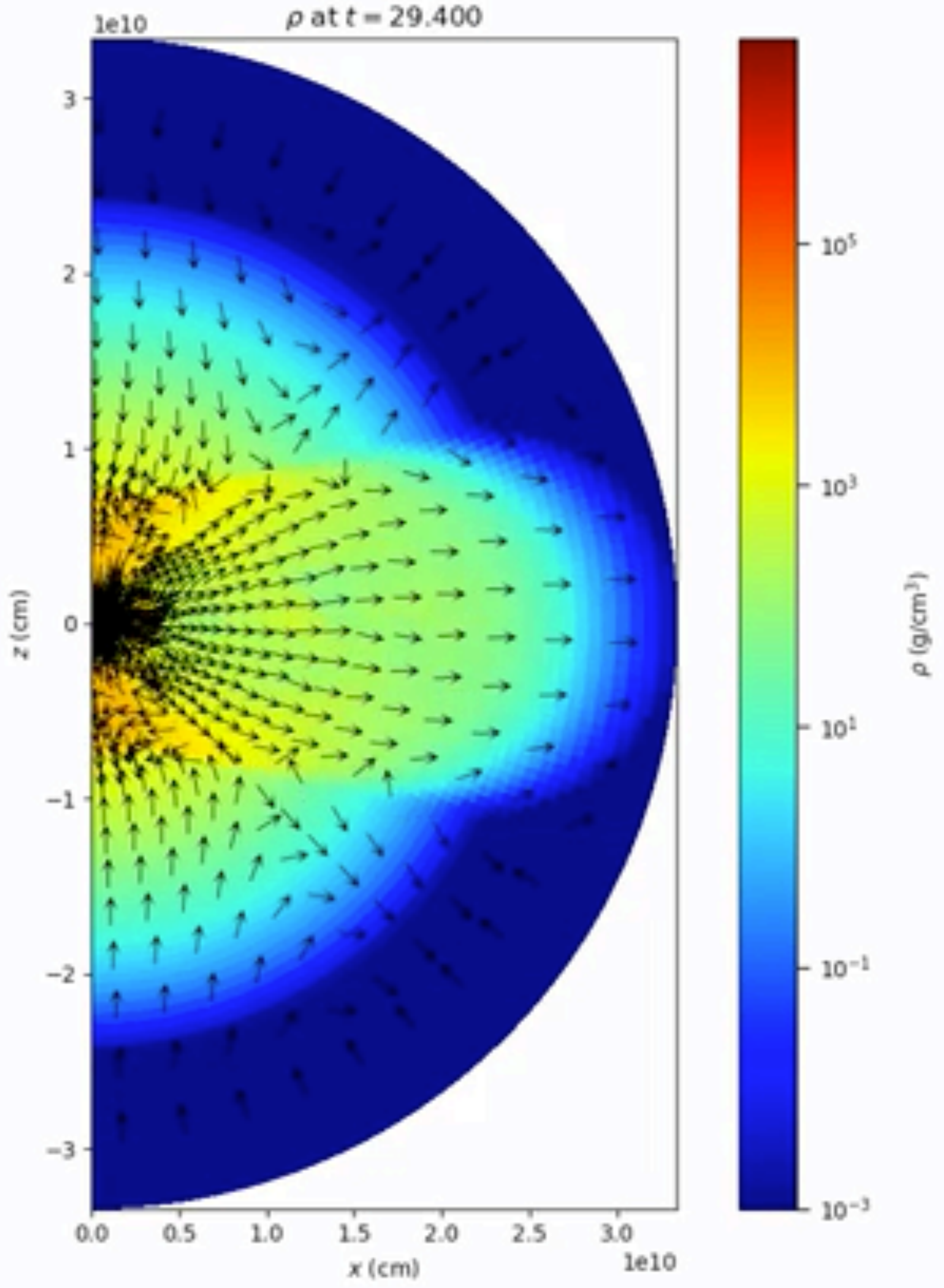

E_{expl} and E_{inj} for different t_w

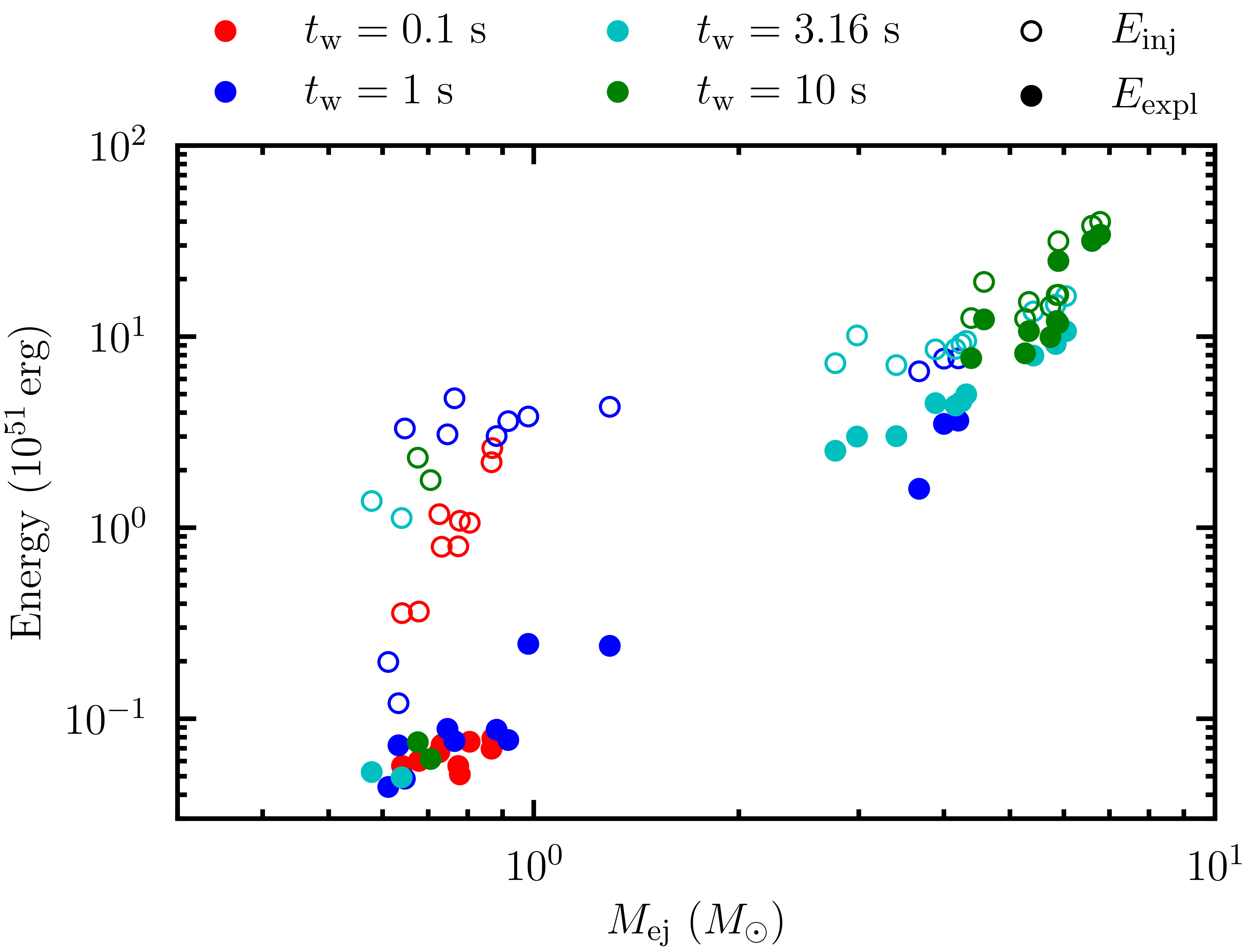

E_{expl} and E_{inj} for different t_w

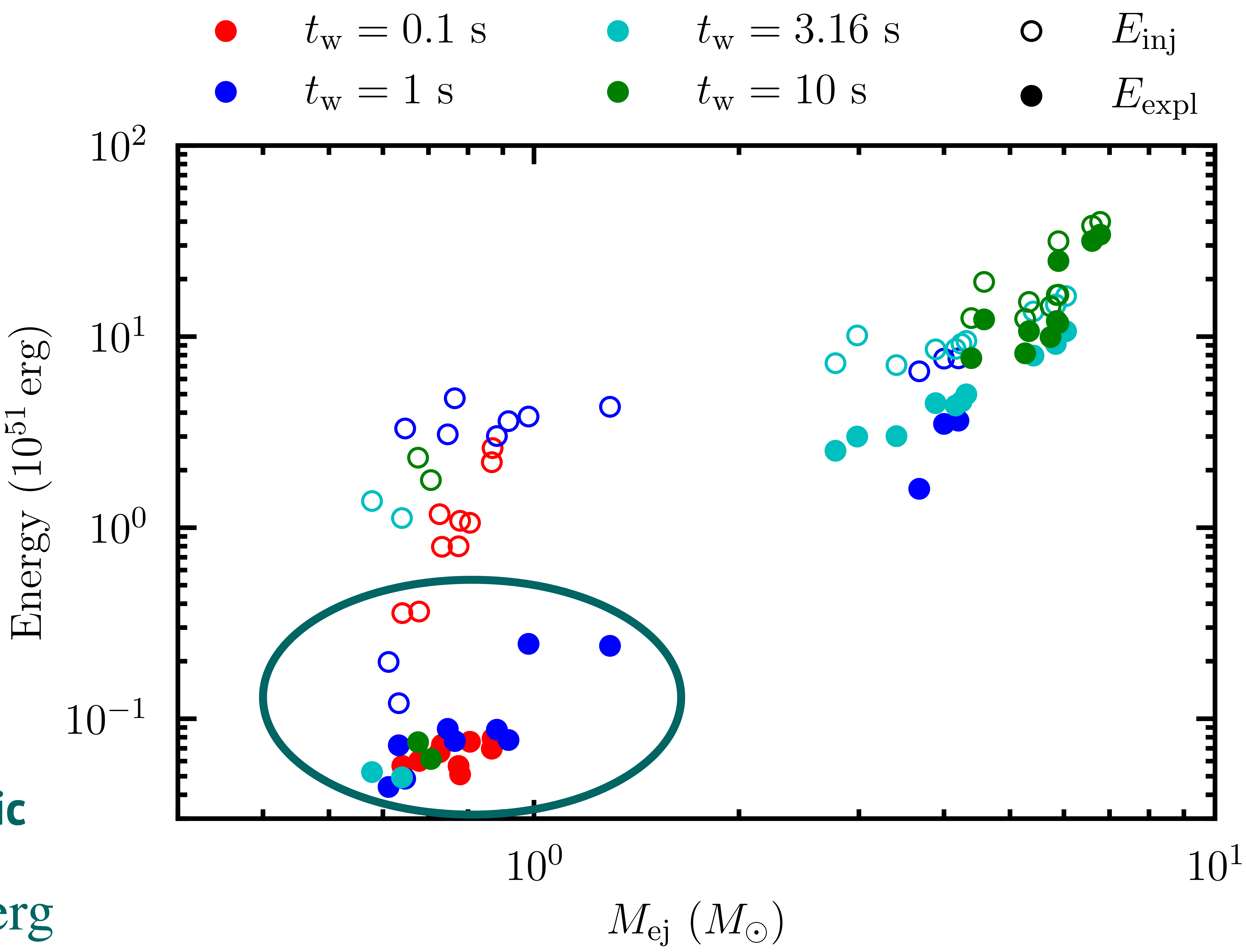

Sub-energetic explosions

$E_{expl} \sim 10^{50}$ erg

E_{expl} and E_{inj} for different t_w

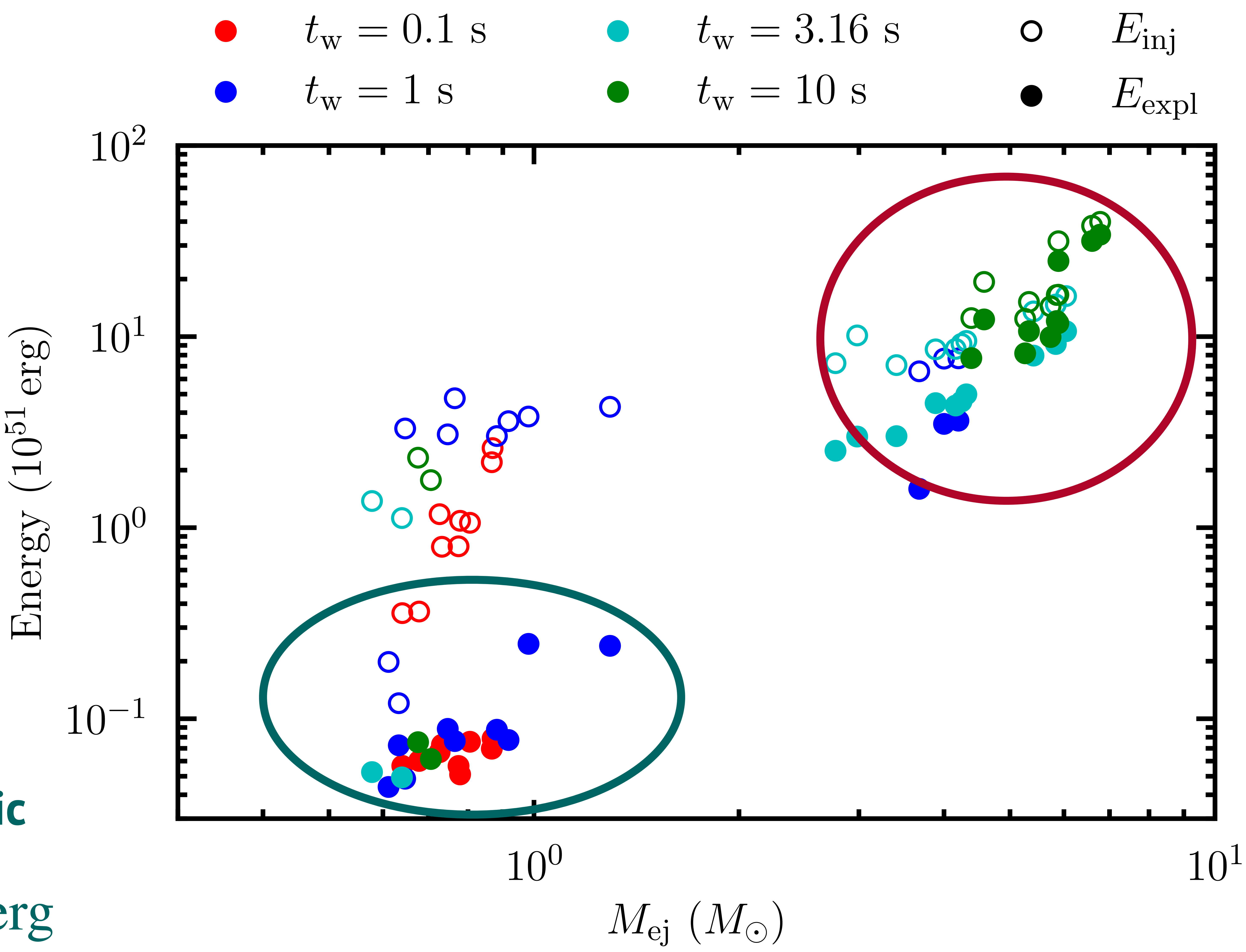

Sub-energetic explosions
$E_{expl} \sim 10^{50}$ erg

Highly-energetic explosions
$E_{expl} \sim 10^{52}$ erg

$E_{\rm expl}$ and $E_{\rm inj}$ for different $t_{\rm w}$

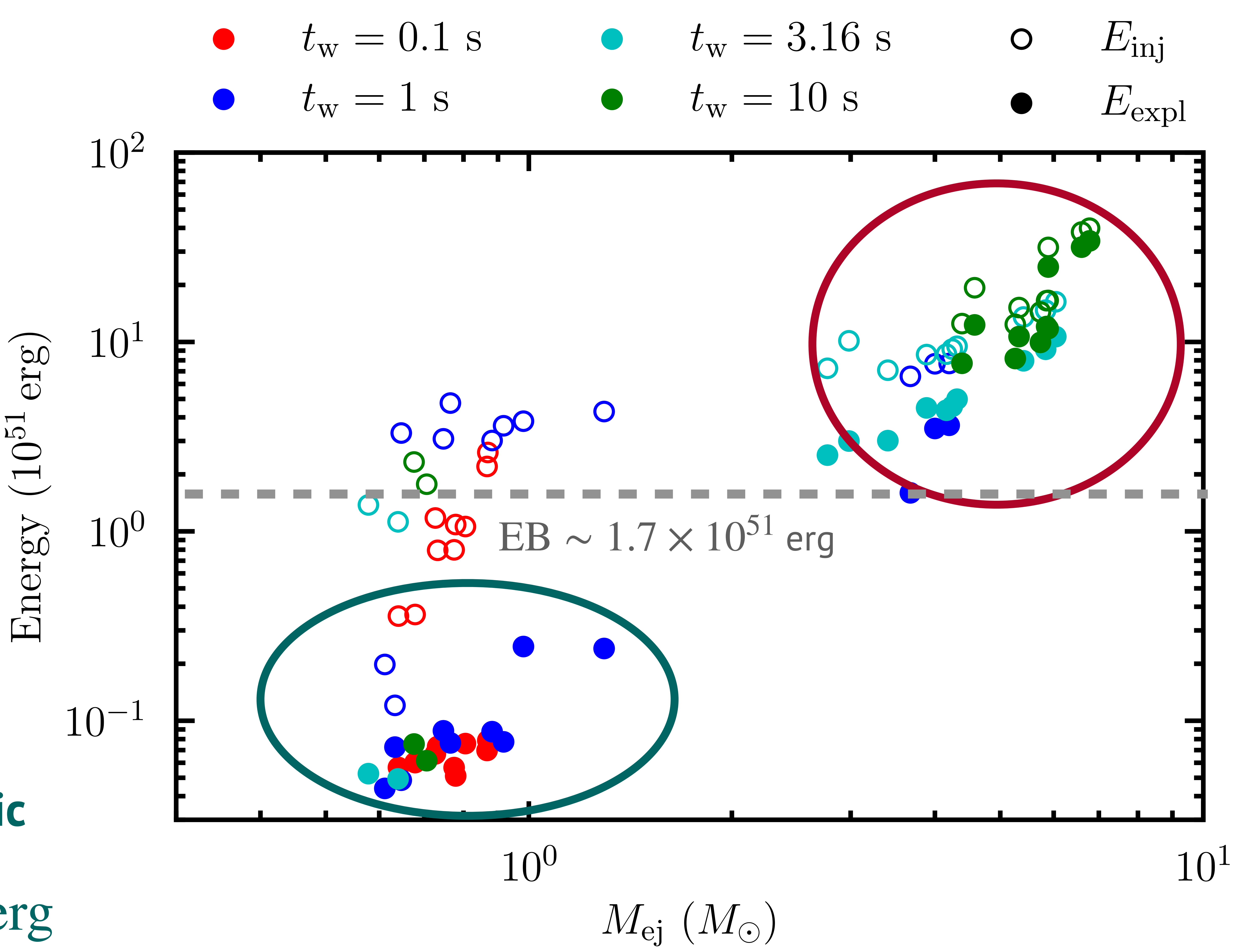

Sub-energetic explosions
$E_{\rm expl} \sim 10^{50}$ erg

Highly-energetic explosions
$E_{\rm expl} \sim 10^{52}$ erg

Two explosion mechanisms

$$E_{\mathrm{expl}} \sim 10^{52}\,\mathrm{erg}$$

Ram pressure dominates and the injected matter can expand outward without falling back

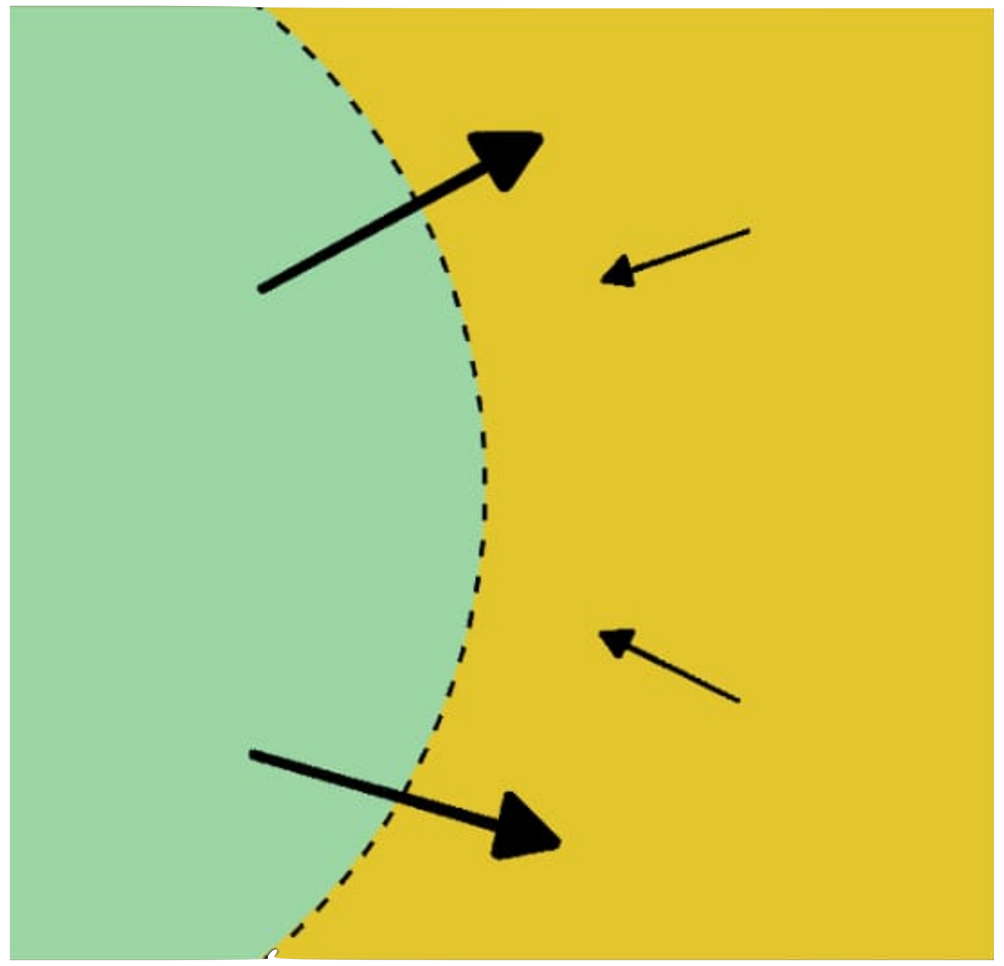

$$E_{\mathrm{expl}} \sim 10^{50}\,\mathrm{erg}$$

Ram pressure is weak and the infalling envelope bounces on the wind, launching the shockwave propagating outward

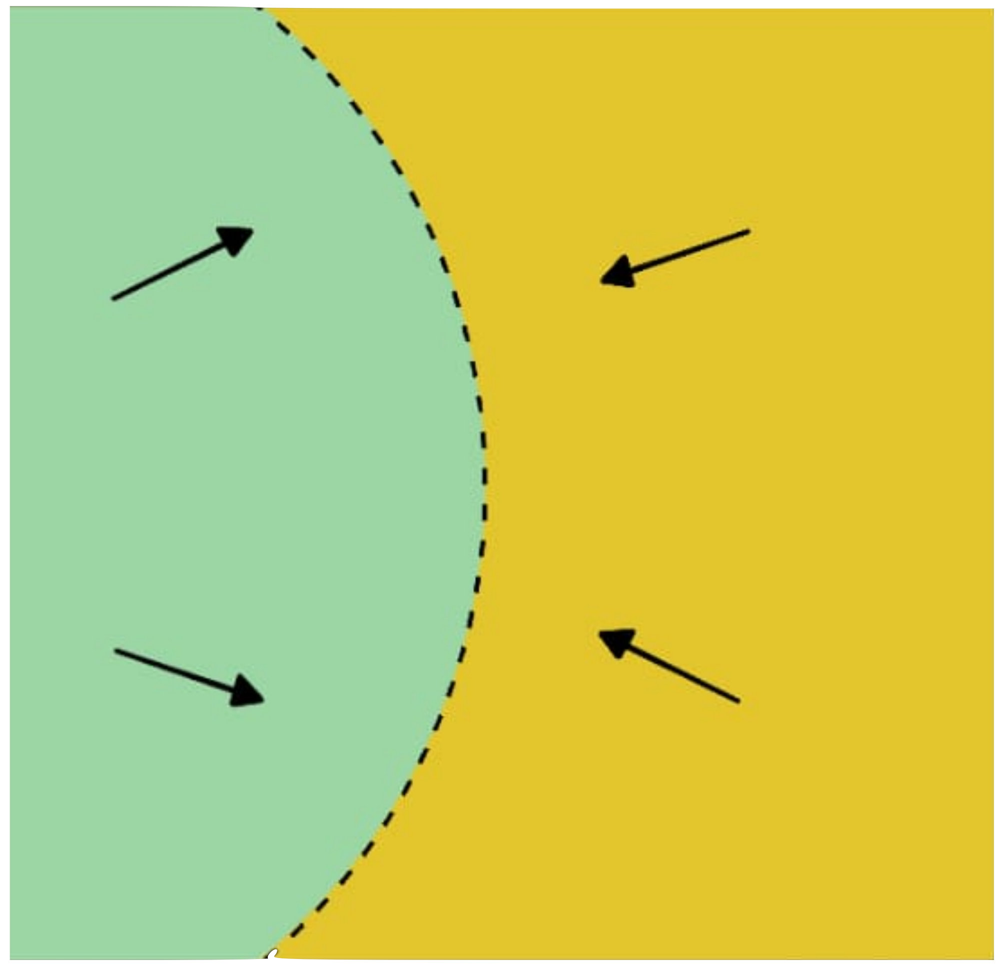

Two explosion mechanisms

$E_{\rm expl} \sim 10^{52}\,{\rm erg}$

The explosion is wind-driven

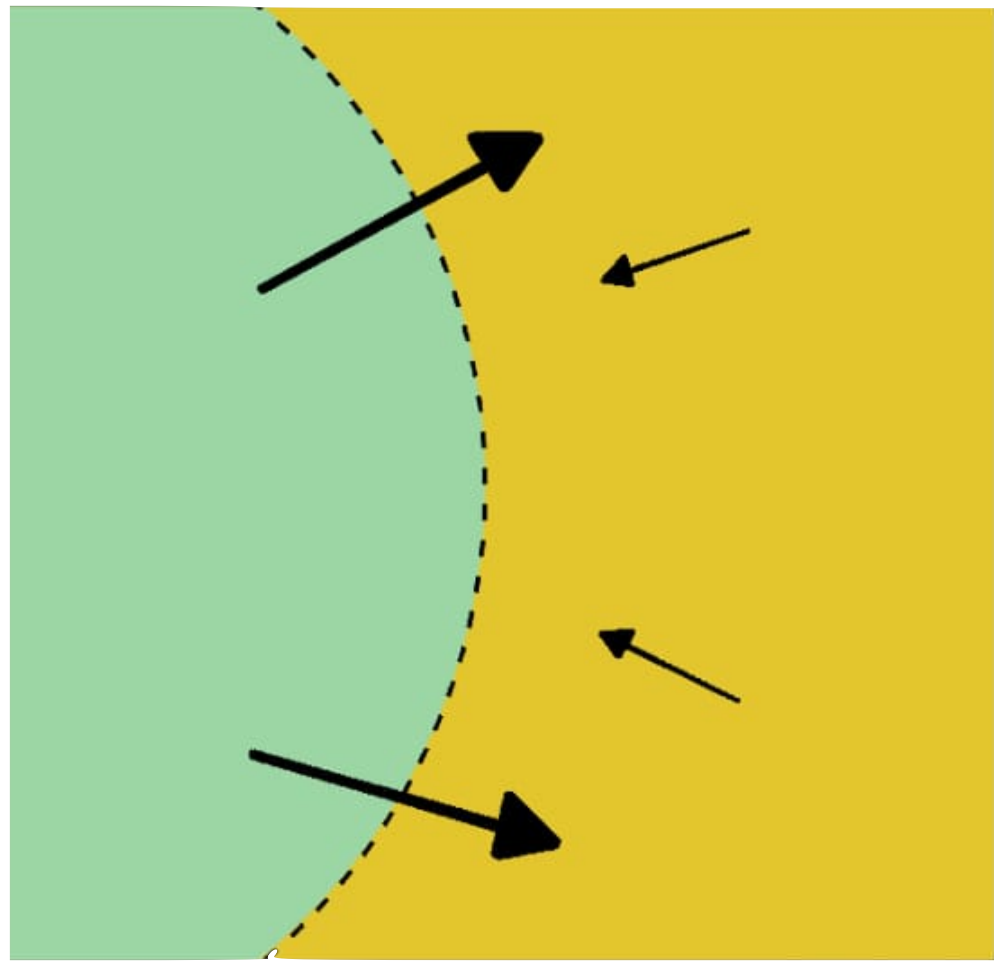

$E_{\rm expl} \sim 10^{50}\,{\rm erg}$

The source of the explosion is the binding energy

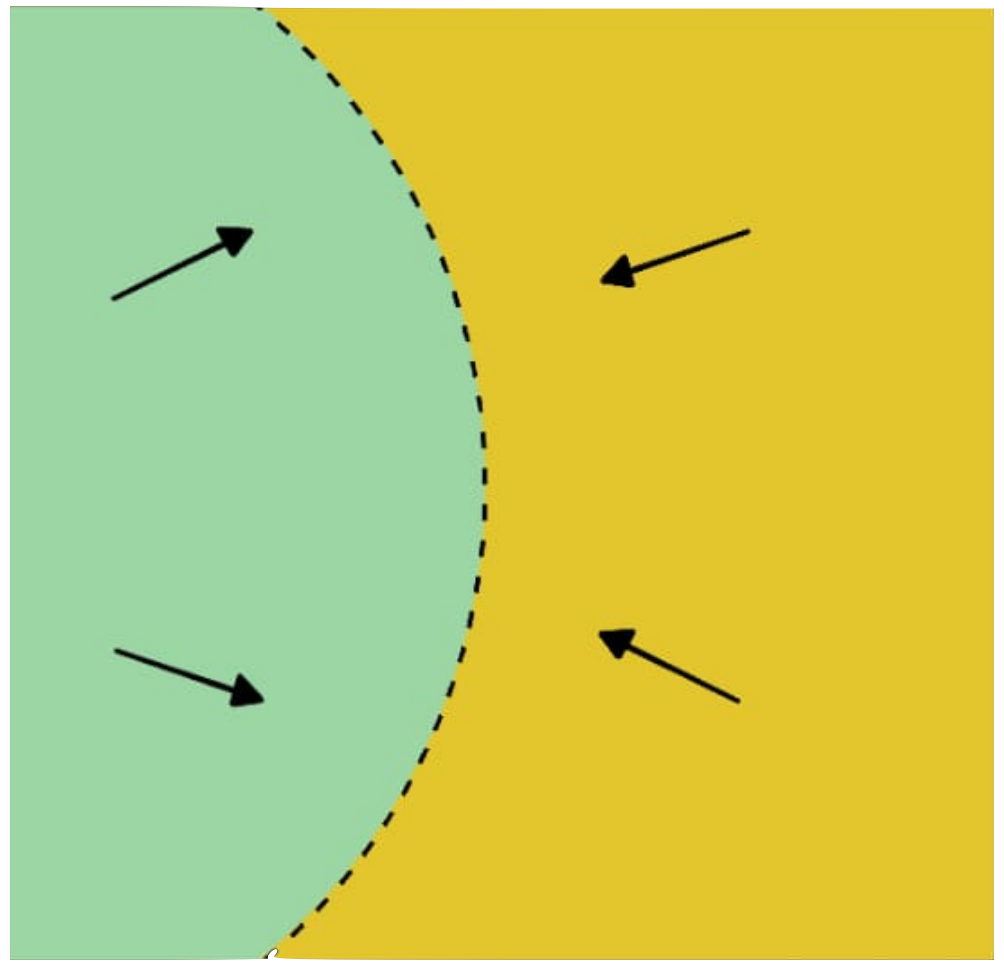

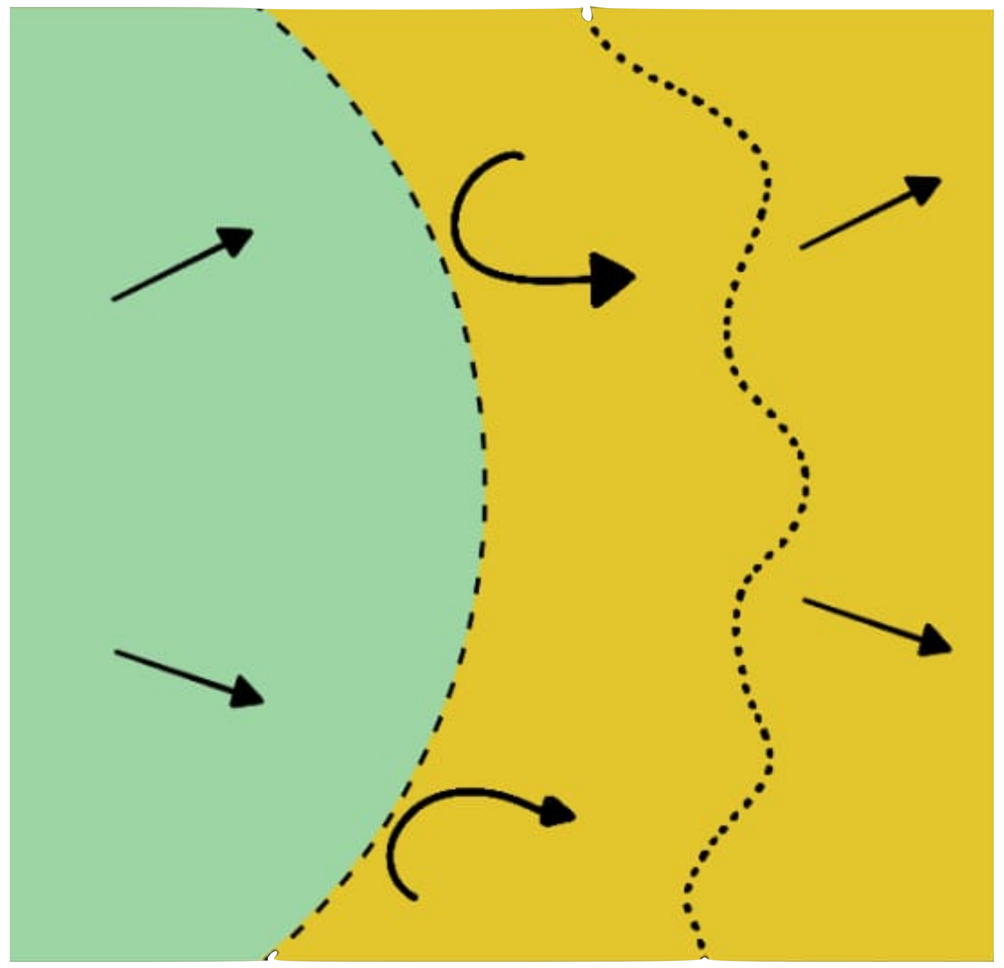

$E_{\rm expl}$ and $E_{\rm inj}$ for different $t_{\rm w}$

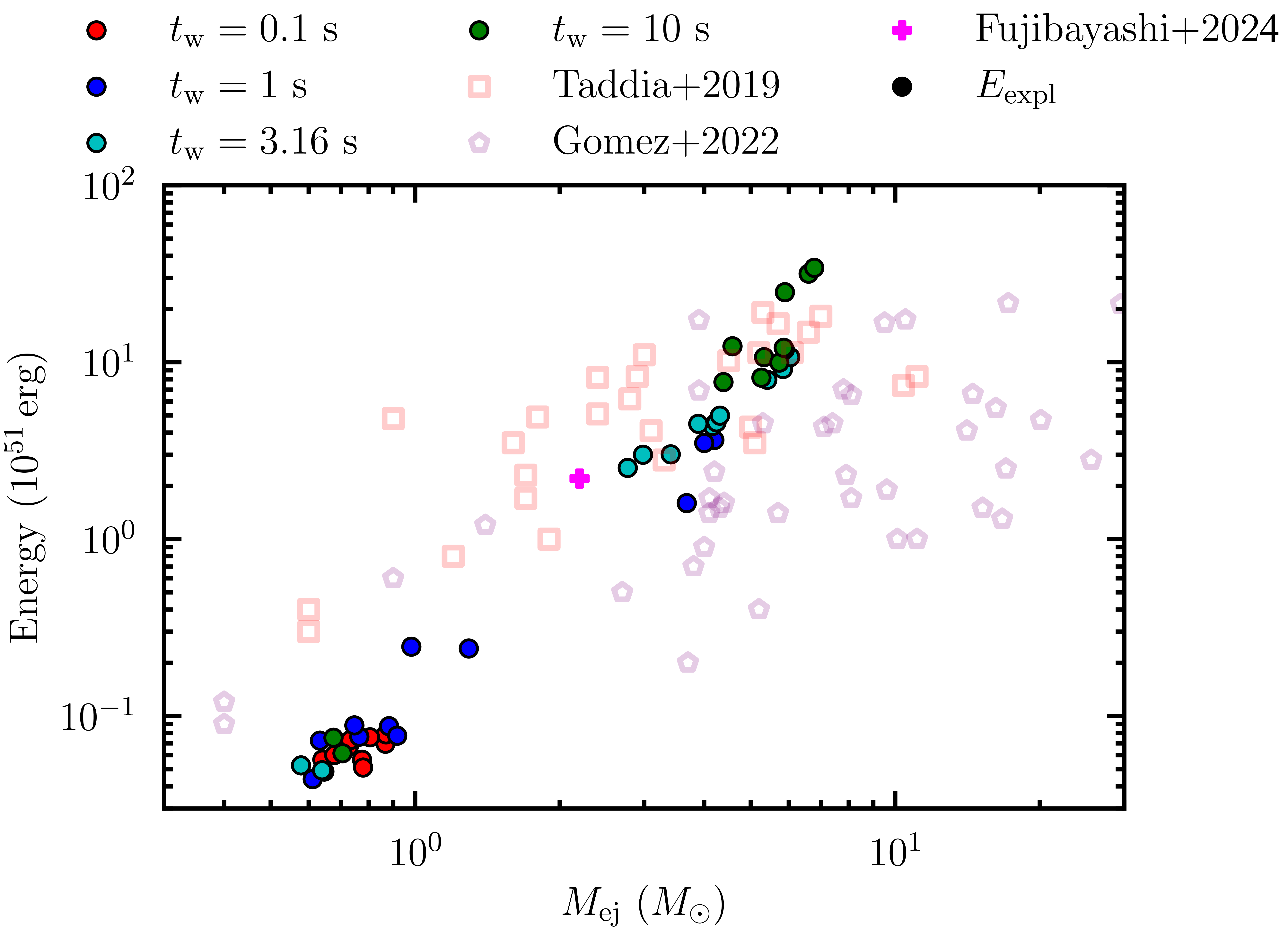

^{56}Ni production

Thermodynamic history of the ejecta with tracer particles following Fujibayashi et al. (2024)

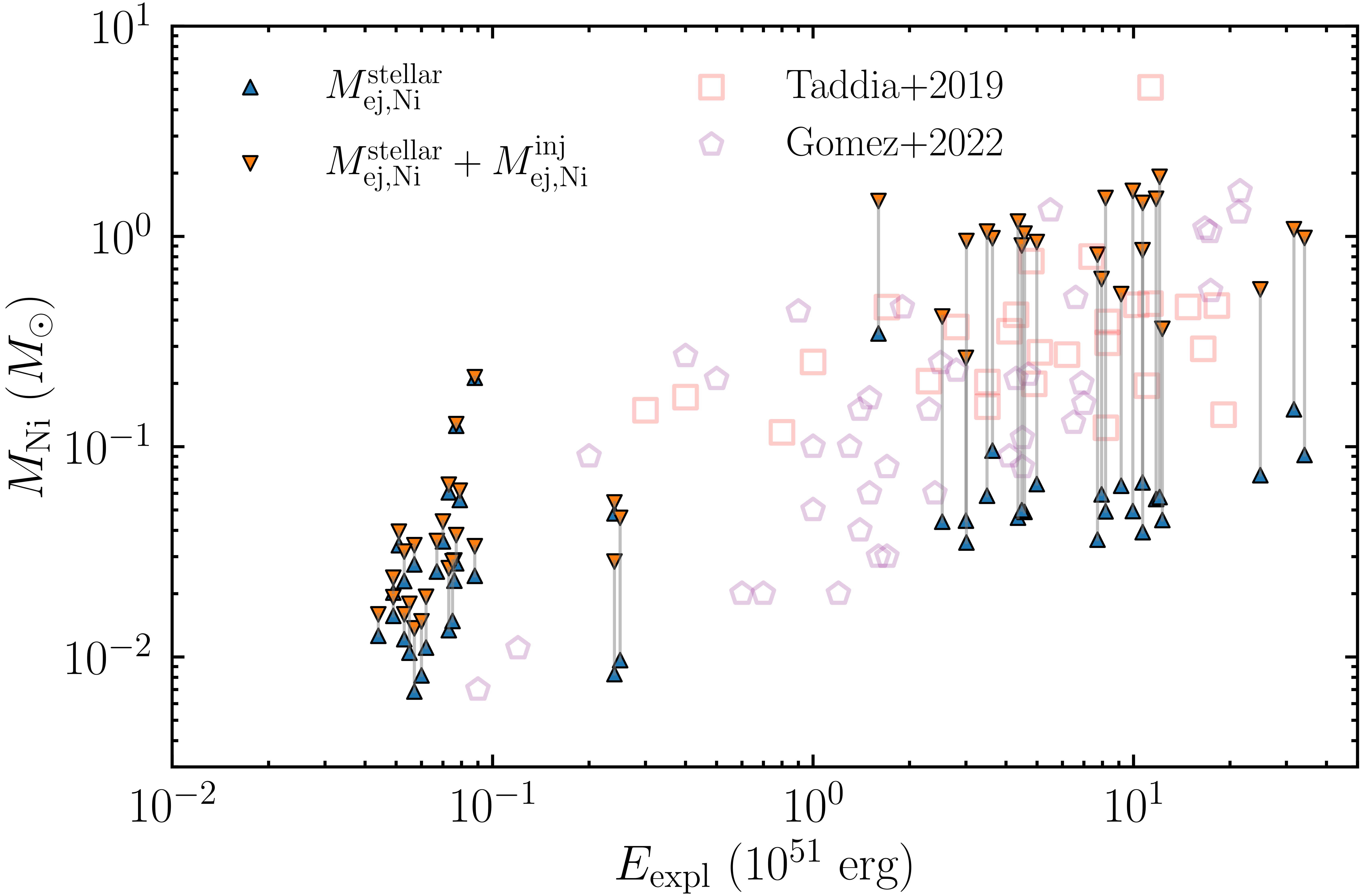

Conclusions

Explosion of a rapidly rotating, low metallicity, rotationally mixed quasi-chemically homogeneous star with $M_{\mathrm{ZAMS}} = 20\,M_{\odot}$ varying the injection parameters

Conclusions

Explosion of a rapidly rotating, low metallicity, rotationally mixed quasi-chemically homogeneous star with $M_{\rm ZAMS} = 20\,M_\odot$ varying the injection parameters

- Wide range of $E_{\rm expl}$ (from $\leq 10^{50}$erg to $\geq 10^{52}$erg) with a bimodal distribution, controlled by the competition between ram pressure and infalling matter

Conclusions

Explosion of a rapidly rotating, low metallicity, rotationally mixed quasi-chemically homogeneous star with $M_{\rm ZAMS} = 20\,M_\odot$ varying the injection parameters

- Wide range of $E_{\rm expl}$ (from $\leq 10^{50}$erg to $\geq 10^{52}$erg) with a bimodal distribution, controlled by the competition between ram pressure and infalling matter

- Longer $t_{\rm w}$ $\rightarrow$ higher mass-infall rate $\rightarrow$ larger $E_{\rm expl}$

Conclusions

Explosion of a rapidly rotating, low metallicity, rotationally mixed quasi-chemically homogeneous star with $M_{\mathrm{ZAMS}} = 20\,M_\odot$ varying the injection parameters

- Wide range of E_{expl} (from $\leq 10^{50}$erg to $\geq 10^{52}$erg) with a bimodal distribution, controlled by the competition between ram pressure and infalling matter
- Longer t_{w} $\rightarrow$ higher mass-infall rate $\rightarrow$ larger E_{expl}
- Nucleosynthesis: measure $> 2.1\,M_\odot$ of ^{56}Ni in high-energy explosions

Conclusions

Explosion of a rapidly rotating, low metallicity, rotationally mixed quasi-chemically homogeneous star with $M_{\rm ZAMS} = 20\,M_\odot$ varying the injection parameters

- Wide range of $E_{\rm expl}$ (from $\leq 10^{50}$erg to $\geq 10^{52}$erg) with a bimodal distribution, controlled by the competition between ram pressure and infalling matter
- Longer $t_{\rm w}$ $\rightarrow$ higher mass-infall rate $\rightarrow$ larger $E_{\rm expl}$
- Nucleosynthesis: measure $> 2.1\,M_\odot$ of ^{56}Ni in high-energy explosions
- Agreement with observational data for Type Ic-BL SNe

Conclusions

Explosion of a rapidly rotating, low metallicity, rotationally mixed quasi-chemically homogeneous star with $M_{\rm ZAMS} = 20\,M_\odot$ varying the injection parameters

- Wide range of $E_{\rm expl}$ (from $\leq 10^{50}$erg to $\geq 10^{52}$erg) with a bimodal distribution, controlled by the competition between ram pressure and infalling matter
- Longer $t_{\rm w}$ $\rightarrow$ higher mass-infall rate $\rightarrow$ larger $E_{\rm expl}$
- Nucleosynthesis: measure $> 2.1\,M_\odot$ of ^{56}Ni in high-energy explosions
- Agreement with observational data for Type Ic-BL SNe
- Agreement with numerical result of Fujibayashi+2024

TeV Particle Astrophysics
TeVPA 2026
Tendo Japan
August 30 - September 4, 2026

ありがとうございました

Thank you

Ludovica Crosato Menegazzi

DESY